UNIVERSIDADE DA BEIRA INTERIOR
Ciências

Novel therapeutic approaches for skin regeneration

Sofia Mendes Saraiva

Dissertação para obtenção do Grau de Mestre em
Bioquímica
(2º ciclo de estudos)

Orientador: Professor Doutor Ilídio Joaquim Sobreira Correia
Coorientadores: Professora Doutora Paula Isabel Teixeira Gonçalves Borges
Mestre Maximiano José Prata Ribeiro

Covilhã, outubro de 2014

UNIVERSIDADE DA BEIRA INTERIOR
Ciências

Novas abordagens terapêuticas para a regeneração da pele

Sofia Mendes Saraiva

Dissertação para obtenção do Grau de Mestre em
Bioquímica
(2º ciclo de estudos)

Orientador: Professor Doutor Ilídio Joaquim Sobreira Correia
Coorientadores: Professora Doutora Paula Isabel Teixeira Gonçalves Borges
Mestre Maximiano José Prata Ribeiro

Covilhã, outubro de 2014

To my parents and my brother…

Acknowledgments

First, I would like to thank to Professor Ilídio Correia for the possibility of developing my master thesis in his group, the unconditional support, guidance and for the patience. During this master thesis Professor Ilídio helped me to grow as an investigator but also as a person. As he says, we have to work hard every single day to achieve our goals. Thank you for all the understanding during all the difficult times.

I thank to Maximiano Ribeiro, my co-supervisor, for his support, guidance and for being a friend. All the advices were very important to overcome the difficulties.

I would also like to thank Sónia Miguel not only for her help in acquiring scanning electron microscopy images of the hydrogels, but also for all the guidance since the beginning of this work, endless support and for being such a comprehensive partner and friend.

Moreover, I would like to thank to my group colleagues for their support and knowledge sharing, at any time. To Ricardo Fradique, Mariana Vallejo and specially Elisabete Costa, thank you for the support, the funny moments and the company during the endless days and nights of work. To Vitor Gaspar, thank you for all the help and patience.

To my closest friends that accompanied me during the academic life. Tânia Pascoal, João Salvado and Sara Maruje, thank you for all the help, support and encouragement during all these years and specially this one. A huge and special thank to Raquel Tavares, whose friendship remained during all these years and no matter what she always there.

Finally, and foremost, a very special thanks to my parents José and Rosa Saraiva and my brother Francisco Saraiva for their unlimited and unconditional support, patience, love and affection. Thank you for never stop believing in me, for making me a strong and better person every day. Nothing would matter without them on my side. To them I dedicate this thesis.

Abstract

The integrity of skin, as the largest organ of the human body, must be preserved in order to play its role as a protective barrier, in the maintenance of fluid homeostasis and temperature regulation. Skin lesions can occur due to different causes, being burns those responsible for extensive skin loss, infection, electrolyte imbalances and respiratory failure. In order to decrease the effects of skin damages, new skin substitutes have been developed to accelerate the healing process and thus restore the native structure of skin. Among the existent materials, hydrogels own the most desirable characteristics of an "ideal dressing", such as biocompatibility and biodegradability. Currently, new photocrosslinkable hydrogels have been developed for tissue engineering purposes. Taking into account the intrinsic properties of hydrogels, the work plan developed during this master thesis allowed the production of photocrosslinkable hydrogels, composed of chitosan and gelatine that present some of the properties required for wound regeneration. Initially, methacrylate groups were added to the chitosan and gelatine primary amine groups, leading to the synthesis of methacrylamide chitosan (MAC) and methacrylamide gelatine (MAG). The chemical modification of the polymers was confirmed by proton nuclear magnetic resonance (^{1}H NMR). Then, MAC and MAG hydrogels were produced using ultraviolet (UV) light in the presence of a photoinitiator (Irgacue 2959). The hydrogels were subsequently characterized by scanning electron microscopy and Fourier transform infrared spectroscopy. Porosity and swelling properties were also analyzed and revealed that the hydrogels with a higher content of chitosan had higher porosity and swelling capacity. The cytotoxic profile of the hydrogels was evaluated through an MTS assay, using human fibroblast cells. Cell adhesion on the surface of the hydrogels was visualized through scanning electron microscopy. The results obtained demonstrated that the hydrogels developed herein possess suitable properties for being used as wound dressings. Therefore, in the future *in vivo* studies will be performed to evaluate the histocompatibility of the hydrogels and their capacity to improve the wound healing process. In addition, growth factors and antimicrobial agents can be incorporated in the hydrogels, in order to improve wound repair and prevent bacterial infections, respectively.

Keywords

Biocompatibility, Hydrogel, *In vitro* studies, Photopolymerization, Wound healing.

Resumo

A pele é o maior órgão do corpo humano e devido ao seu papel protetor, regulador da temperatura do corpo e manutenção da homeostase de líquidos, a sua integridade estrutural deve ser preservada de forma a desempenhar corretamente as suas funções. As lesões na pele podem ser causadas por diferentes fatores, sendo as queimaduras a causa mais comum. A perda da integridade estrutural do sistema tegumentar pode provocar a desidratação do doente, infeções, distúrbios eletrolíticos e falhas respiratórias. Com o intuito de ultrapassar os problemas associados às lesões cutâneas, têm sido desenvolvidos novos substitutos de pele que permitam acelerar o processo de cicatrização e assim restaurar a estrutura nativa da pele. De entre os materiais existentes, os hidrogéis são os que possuem as características mais adequadas para serem usados como substitutos de pele. Na atualidade, novos hidrogéis fotopolimerizáveis têm sido desenvolvidos para serem usados na área da engenharia de tecidos. Tendo em conta as propriedades intrínsecas deste tipo de hidrogéis, no presente plano de trabalhos foram desenvolvidos hidrogéis fotopolimerizáveis constituídos por quitosano e gelatina, com o intuito de serem usados na regeneração de feridas. Inicialmente, grupos metacrilato foram incorporados nas aminas primárias do quitosano e da gelatina, permitindo a síntese do quitosano metacrilamida (MAC) e da gelatina metacrilamida (MAG). A modificação dos polímeros foi confirmada através de ressonância magnética nuclear (^{1}H NMR). Os hidrogéis MAC e MAG foram produzidos na presença de um fotoiniciador (Irgacure 2959), usando luz ultravioleta (UV). Os hidrogéis foram caracterizados por microscopia eletrónica de varrimento e espetroscopia de infravermelho com transformada de Fourier. A porosidade e capacidade dos hidrogéis absorverem água também foram analisadas, demonstrando que o hidrogel com maior teor de quitosano apresentava maior porosidade e capacidade de absorção de água. O perfil citotóxico dos hidrogéis foi avaliado através de ensaios MTS, usando fibroblastos humanos como células modelo. A adesão celular na superfície dos hidrogéis foi visualizada através de microscopia eletrónica de varrimento. Os resultados obtidos demonstraram que os hidrogéis desenvolvidos possuem propriedades adequadas para serem usados na regeneração de feridas. No futuro, serão efetuados testes *in vivo* para avaliar a histocompatibilidade dos hidrogéis e a sua capacidade para promover o processo de regeneração de feridas. Fatores de crescimento e agentes antimicrobianos podem ser incorporados nos hidrogéis, por forma a melhorar o processo de regeneração e prevenir infeções bacterianas, respetivamente.

Palavras-chave

Biocompatibilidade, Cicatrização de feridas, Estudos *in vitro*, Fotopolimerização, Hidrogel.

Resumo alargado

A pele é o maior órgão do corpo humano, apresentando uma área aproximada de 2 m^2 nos adultos. Devido ao seu papel protetor, regulador da temperatura do corpo e manutenção da homeostase de líquidos, a sua integridade estrutural deve ser preservada de forma a desempenhar corretamente as suas funções. As lesões da pele são o resultado da disrupção da sua estrutura anatómica e podem ser causadas por diferentes fatores, sendo as queimaduras a causa mais comum. A perda da integridade estrutural do sistema tegumentar pode provocar a desidratação do doente, infeções, distúrbios eletrolíticos e falhas respiratórias.

Consoante o tipo e duração do processo de cicatrização das feridas, as lesões da pele podem ser classificadas como agudas ou crónicas. A cicatrização de feridas é realizada através de uma cascata de eventos complexos e dinâmicos, que incluem a coagulação, inflamação, síntese e deposição de matriz extracelular, angiogénese, fibroplasia, epitelização, contração e remodelação. Após a ocorrência de uma lesão a pele deve ser revestida, a fim de diminuir a dor e o risco de infeção e promover o restabelecimento da sua integridade, minimizando assim a perda das suas funções. A terapêutica "standard" para o tratamento da perda de grandes quantidades de pele, por exemplo devido a queimaduras, continua a ser o uso de auto-, alo- e xeno-enxertos. Contudo esta abordagem terapêutica apresenta limitações como rejeição e transmissão de doenças. Para colmatar estas limitações, nas últimas décadas, vários substitutos de pele têm sido desenvolvidos de forma a acelerar o processo de cicatrização e restabelecer as funções da pele.

De acordo com a camada da pele que pretendem substituir, os substitutos de pele podem ser classificados como epidérmicos, dérmicos e dermo-epidérmicos. Os substitutos de pele podem ser constituídos à base de polímeros naturais e/ou sintéticos, sendo que alguns possuem ainda células. Contudo, nenhum dos substitutos atualmente disponíveis no mercado é capaz de reestabelecer totalmente as propriedades funcionais e anatómicas da pele.

De entre os materiais existentes, os hidrogéis são os que possuem as características que mais se enquadram nas propriedades de um "substituto ideal", uma vez que são biocompatíveis e biodegradáveis, apresentam uma estrutura semelhante à da matriz extracelular e têm a capacidade de prevenir a desidratação da ferida e de remover exsudados. Além disso, alguns hidrogéis são particularmente interessantes devido à possibilidade de serem formados *in situ* e aplicados através de processos minimamente invasivos, como é o caso dos hidrogéis fotopolimerizáveis.

A aplicação de materiais fotopolimerizáveis tem sido extensivamente usada em medicina dentária devido à rápida reticulação dos materiais sob uma breve exposição à luz ultravioleta.

Recentemente, os hidrogéis fotopolimerizáveis têm sido alvo de grande atenção na engenharia de tecidos devido à sua biocompatibilidade, rápida reticulação e aplicação *in situ*. A fotopolimerização permite ainda controlar a estrutura dos materiais, produzindo hidrogéis com as propriedades mecânicas desejadas.

O presente plano de trabalhos teve como objetivo o desenvolvimento de hidrogéis fotopolimerizáveis, constituídos por quitosano e gelatina, com o intuito de serem aplicados na regeneração de feridas. Estes polímeros naturais foram usados devido ao seu baixo custo, biocompatibilidade e biodegradabilidade, e pelo fato de não induzirem uma resposta imunológica. Inicialmente, grupos metacrilato foram adicionados às aminas primárias do quitosano e da gelatina, permitindo a síntese do quitosano metacrilamida (MAC) e da gelatina metacrilamida (MAG). A modificação dos polímeros foi confirmada e determinada através de ressonância magnética nuclear (^{1}H NMR). Os hidrogéis MAC e MAG foram produzidos na presença de um fotoiniciador (Irgacure 2959), usando luz ultravioleta (UV). O Irgacure 2959 foi usado como iniciador uma vez que é conhecido pela baixa toxicidade para as células.

Os hidrogéis foram caracterizados por microscopia eletrónica de varrimento e espetroscopia de infravermelho com transformada de Fourier. A porosidade e capacidade dos hidrogéis absorverem água também foram analisadas, demonstrando que o hidrogel com maior teor de quitosano apresentava maior porosidade e capacidade de absorção de água. O perfil citotóxico dos hidrogéis foi avaliado *in vitro* através de ensaios MTS, usando fibroblastos humanos como células modelo. A adesão celular na superfície dos hidrogéis foi visualizada através de microscopia eletrónica de varrimento. Os resultados obtidos demonstraram que o hidrogel com mais quitosano apresenta uma estrutura mais porosa e com maior capacidade de absorção de água. Os hidrogéis revelaram ser biocompatíveis e capazes de promover a adesão e proliferação dos fibroblastos. Tais resultados sugerem que os hidrogéis fotopolimerizáveis desenvolvidos possuem propriedades adequadas para serem usados na regeneração de feridas. No futuro, serão realizados testes *in vivo* para avaliar a histocompatibilidade dos hidrogéis e a sua capacidade para promover o processo de regeneração de feridas. Fatores de crescimento e agentes antimicrobianos podem ser incorporados nos hidrogéis, por forma a melhorar o processo de regeneração e prevenir infeções bacterianas, respetivamente.

Index

Chapter III - Results and Discussion

Chapter IV - Conclusion and Future Perspectives

Chapter V - References

Figure Index

Chapter I - Introduction

Chapter III - Results and Discussion

Table Index

List of abbreviations

1DUVS	First derivative UV-spectroscopy
3D	Three-dimensional
APS	Ammonium persulfate
Az-CH-LA	Azidobenzoic acid-modified lactose chitosan
BSA	Bovine serum albumin
DD	Degree of deacetylation
DM	Degree of methacrylation
DMEM-F12	Dulbecco's modified Eagle's medium
ECM	Extracelular matrix
EDTA	Ethylenediaminetetraacetic acid
FBS	Fetal bovine serum
FGF	Fibroblast growth factor
FTIR	Fourier transform infrared spectroscopy
GAGs	Glycosaminoglycans
GFs	Growth factors
HA	Hyaluronic acid
HAM	Hyaluronic acid membrane
Irgacure 2959	2-hydroxy-1-(4-(hydroxyethoxy)phenyl)-2-methyl-1-propanone
K^-	Negative Control
K^+	Positive Control
MA	Methacrylic anhydride
MAC	Methacrylamide chitosan
MAG	Methacrylamide gelatine
MMPs	Metalloproteinases
MMW	Medium molecular weight

MTS	3-(4,5-dimethylthiazol-2-yl)-5-(3-carboxymethoxyphenyl)-2-(4-sulfophenyl) -2H-tetrazolium
NHDF	Normal Human Dermal Fibroblasts
NIH-3T3	Mouse embryonic fibroblast
NMR	Nuclear Magnetic Ressonance
PAM	Polyacrylamide
PBS	Phosphate-buffered saline solution
PDGF	Platelet-derived growth factor
PEG	Poly(ethylene glycol)
PEO	Poly(ethylene oxide)
PGA	Poly(glycolic acid)
PHEMA	Poly(2-hydroxyethyl methacrylate)
PI	Photoinitiator
PLA	Poly(lactic acid)
PVA	Poly(vinyl alcohol)
RT	Room temperature
SC	Stratum corneum
SEM	Scanning electron microscopy
SMBS	Sodium metabisulfite
TIMP	Tissue inhibitors of metalloproteinases
WHO	World Health Organization
UV	Ultraviolet
VEGF	Vascular endothelial growth factor

Chapter I

Introduction

1. Introduction

1.1. Skin

1.1.1. Functions and structure

Skin is the largest organ of the human body, occupying almost 2 m^2 of surface area and accounting for 7% of body's mass [1]. Its primary function is to serve as a protective barrier against external insults from the environment, such as ultraviolet (UV) light radiation, chemicals and pathogens. Skin is also involved in fluid homeostasis maintenance, thermoregulation, immune surveillance, sensory detection and self-healing [2-5]. Such demands require that the structure of this tissue is not compromised [6]. Moreover, since skin is the outward appearance of an individual to the world, it is also an indicator of well being and health state of the individual [7]. The injuries or diseases that lead to the loss of the integrity of large portions of skin may result in significant morbidity and mortality [4].

The skin has a complex structure (figure 1) and is organized in three distinct layers, known as epidermis, dermis and hypodermis [8]. Associated with the epidermis and dermis are various appendages such as nails, hair follicles, sweat and sebaceous glands, nerves, lymphatic and blood vessels, that play different functions [9, 10].

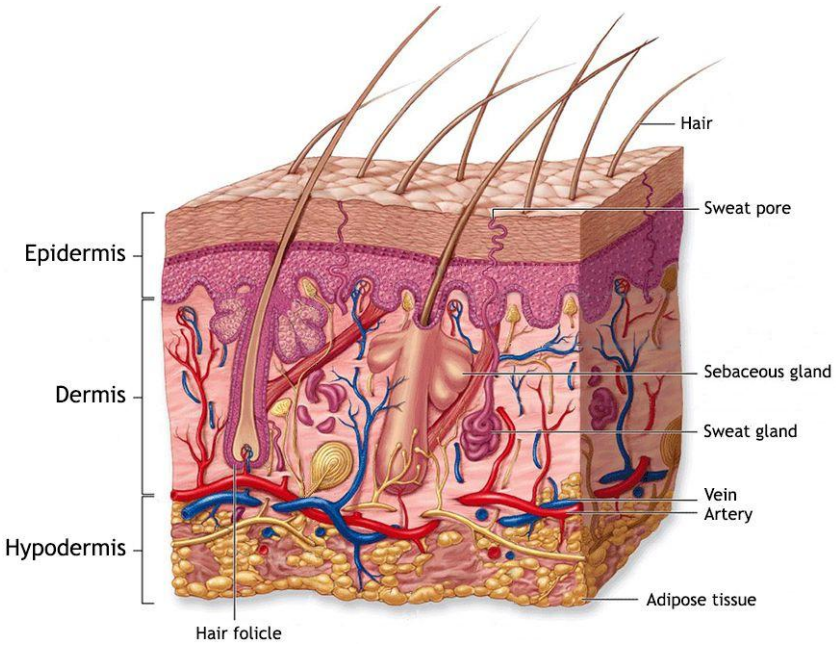

Figure 1: Representation of the structure of the skin (adapted from [11]).

1.1.2. Epidermis

The epidermis is the outermost layer of skin (figure 1) and contains no blood vessels. This stratified layer has evolved to provide a physical barrier that is fundamental for organisms' survival, since it prevents the loss of fluids and infections [9, 12].

keratinocytes are the most abundant cell type in epidermis (90 – 95%). Their ability of undergoing self-renewal through a continuous process of proliferation, differentiation and cell death, enables the compartmentalization of epidermis into different strata (figure 2) that represent different stages of keratinocyte maturation [13]. Epidermal differentiation begins with the migration of keratinocytes from the *stratum basale*, which is the first layer of epidermis counting from the inside to the outside. As the basal keratinocytes proliferate, the "daughter" cells migrate towards and differentiate, forming the other four sub-layers of epidermis, known as [2, 9, 10, 12]:

- *stratum spinosum,* a layer of spinous cells where the keratinization process begins;
- *stratum granulosum,* a granular layer where differentiated keratinocytes become granular cells;
- *stratum lucidum,* a thin and translucent layer of dead cells (mostly seen in palms and soles);
- *stratum corneum* (SC), also known as cornified layer, represents the final result of keratinocyte differentiation. SC is formed by completely differentiated dead keratinocytes (corneocytes) lacking nuclei and organelles, and interspersed with intercellular lipids (mainly ceramides and sphingolipids). This layer provides the most significant contribution to the permeation barrier property of human skin.

Besides keratinocytes, there are other cells that have significant roles in the epidermis. Melanocytes are present in the *stratum basale* and produce melanin, which contributes for skin pigmentation and protects the skin from harmful ultraviolet radiation. Specialized epidermal cells, known as Merkel cells, are also present in the *stratum basale* and are associated with nerve endings that are responsible for detecting superficial pressure. The Langerhan's cells are dendritic cells present in the *stratum spinosum* that have an essential role in the skin immune defence system [9, 10, 14].

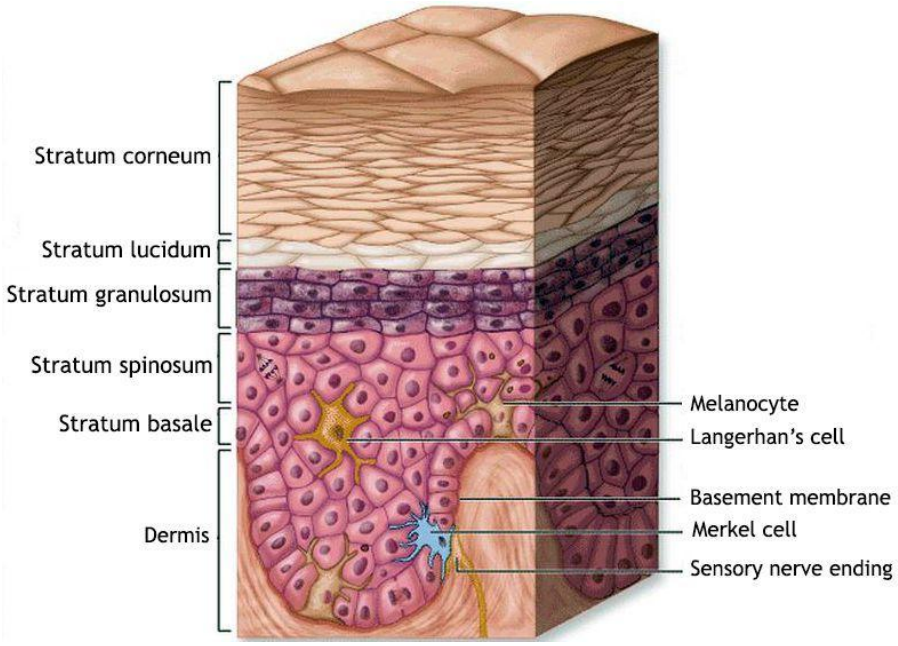

Figure 2: Representation of epidermis layers (adapted from [11]).

The epidermis layer is connected to the underlying dermis via basement membrane, at the dermal-epidermal junction. The basement membrane, can be divided into *lamina lucida,* the layer closer to the epidermis, which is made up of laminin, integrins, entactins, and dystroglycans and *lamina densa,* a sheet-like structure composed mainly of collagen type IV [10, 14].

1.1.3. Dermis

The dermis lies between the epidermis and the hypodermis (figure 1). This skin layer is enriched with nerve fibres, blood and lymphatic vessels [1, 2, 8-10]. The dermis' cellular components include fibroblasts, adipocytes, macrophages and mast cells. Fibroblasts are the major cell type present in the dermis and they are capable of producing different collagens, elastic fibres, glycosaminoglycans, glycoproteins and remodelling enzymes (proteases and collagenases). The collagens and elastic fibres present in the dermis layer confer support and elasticity to the skin [15].

Dermis is divided in papillary and reticular layers. The superficial papillary dermis is composed by thin fibres that are loosely arranged and contains blood vessels that supply the epidermis with nutrients, remove waste products and help in body temperature regulation.

The deeper *reticular dermis* accounts for 80% of dermis and is composed by dense collagen and elastic fibre matrix, conferring strength and flexibility to the skin [1, 14, 15].

1.1.4. Hypodermis

Below the dermis is the hypodermis, also known as subcutaneous tissue, is mainly made up of fat and connective tissues (figure 1). This layer is highly vascularised, providing blood vessels and nerves to the skin and also allowing its connection to the underlying bones and muscles, contributing to the thermoregulatory and mechanical properties of the skin [8, 14].

1.2. Wounds

According to the Wound Healing Society, a wound is the outcome of the "disruption of normal anatomic structure and function" of the skin [16]. Skin lesions are traumatic events that can occur due to several reasons, including genetic disorders, surgical interventions, acute trauma or chronic wounds [17, 18].

Depending on the nature of the repair process, wounds can be classified as acute or chronic wounds. **Acute wounds** include mechanical lesions like abrasions, surgically created wounds and traumatic injuries like burns, among others. Usually this kind of wounds heals completely within 8-12 weeks. Acute wound healing is a timely ordered process that involves a complex series of events, regulated by several mediators such as platelets, inflammatory cells, cytokines and growth factors (GFs) [16, 19, 20]. On the other hand, some wounds fail to heal due to the interruption of the orderly sequence of events of the healing process, caused by the occurrence of an infection or an underlying disease process. These non-healing-wounds, known as **chronic wounds**, require continued management. Decubitis ulcers and leg ulcers are some examples of chronic wounds [16, 20, 21].

Wounds can also be classified according to the extent of surface area and depth involved [17]:

- **Epidermal** – typical of sunburns, light scalds and abrasions. In this type of wounds only the epidermis is affected, and they are characterized by erythema and minor pain. Such injuries will regenerate rapidly without scaring;

- **Superficial partial-thickness** – the epidermis and superficial parts of the dermis are affected, causing severe pain and epidermal blistering like in the case of thermal trauma. Healing will occur through the epithelialization from the margins and the edge of the wound, by keratinocytes;

- **Deep partial-thickness** – a large area of skin is affected. Due to the depth of the injury, it will require long periods to heal and the scaring will be more pronounced than in the case of superficial partial-thickness wounds;

- **Full-thickness** – there is a complete destruction of the skin appendages. Such injuries heal by contraction, and the epithelialization process occurs only from the edge of the wound. Since these injuries cannot epithelialize on their own, they require skin grafting and may lead to cosmetic (extensive scaring) and functional defects.

1.2.1 Types of wound healing

Skin lesions lead to the increase of fluid loss, hypothermia, locally immunocompromised regions, infections and scarring that causes the change of body image [22]. Due to the crucial role of skin in maintaining the homeostasis, its integrity must be restored [20].

The mode of repair is primarily resultant from the depth of the injury [20, 21]:

- **Primary healing** occurs when a wound, created by laceration or surgical incision, causes only focal disruption of the continuity of the epithelial basement membrane. The wound is closed within 12-24 h of its occurrence;

- **Delayed primary healing** involves wounds that remain open for some days as a consequence of bacterial contamination. The closure is performed after the debridment by host defences. After 3-4 days, phagocytic and inflammatory cells are recruited to the wound site to fight and eliminate the cause of the infection. Collagen metabolism is usually unaffected and the wound retains its tensile strength;

- **Secondary healing** occurs when the wound edges cannot be approximated due to the extensive loss of soft tissue, caused by a major trauma like severe burns and some surgical procedures. This type of wound healing is common in patients with underlying co-morbidities such as vascular, diabetic and pressure ulcers. The wound is left open and thus prone to infections. The epithelial cells aren't capable of restoring the original architecture by themselves and the defect will slowly be filled with granulation tissue.

Myofibroblasts that have structural properties, similar to that of fibroblast and smooth muscle cells, are thought to play a crucial role in the healing of this type of injuries. The secondary healing is slower and may lead to skin functional defects.

1.2.2. Wound healing mechanism

Wound healing is an extremely dynamic, interactive and complex biological process that includes a wide range of mechanisms, such as coagulation, inflammation, matrix synthesis and deposition, angiogenesis, fibroplasia, epithelialization, contraction and remodelling. These mechanisms involve complex interactions of components from extracellular matrix (ECM), GFs, resident cells and infiltrating leukocytes for the re-establishment of the integrity of the damaged tissue [18, 22]. The wound healing process comprises four phases: haemostasis, inflammation, cell migration-proliferation and remodelling (figure 3) [20, 21, 23, 24].

1.2.2.1. Haemostasis

After the occurrence of an injury, haemostasis begins spontaneously. The loss of structural integrity triggers platelet aggregation, fibrin clot formation and activation of the coagulation cascade. Within seconds, vasoconstriction occurs to reduce blood loss (figure 3). The platelets trapped in the clot degranulate and release their alpha granules that secrete several GFs, which in turn will attract and activate fibroblasts, endothelial cells and macrophages. Moreover, the platelet plug confers support to the infiltrating cells [20, 21, 23, 25].

1.2.2.2. Inflammation

The inflammatory phase occurs almost simultaneously with haemostasis (figure 3) and its main purpose is to clean the wound by removing the necrotic tissues and to prevent infection. The activation of coagulation and complement system leads to the release of chemoattractants that recruit neutrophils into the wound site. Once in the wound, they start the phagocytosis of bacteria and kill them by releasing enzymes and free radicals. After 2-3 days, blood monocytes enter to the wound and differentiate into macrophages. These cells play a crucial role in the later stages of inflammation, since they act as phagocytic cells and secrete GFs that are responsible for the proliferation of endothelial and smooth muscle cells and for the production of ECM by fibroblasts. They also release enzymes that help to debride the wound [16, 20, 24, 25].

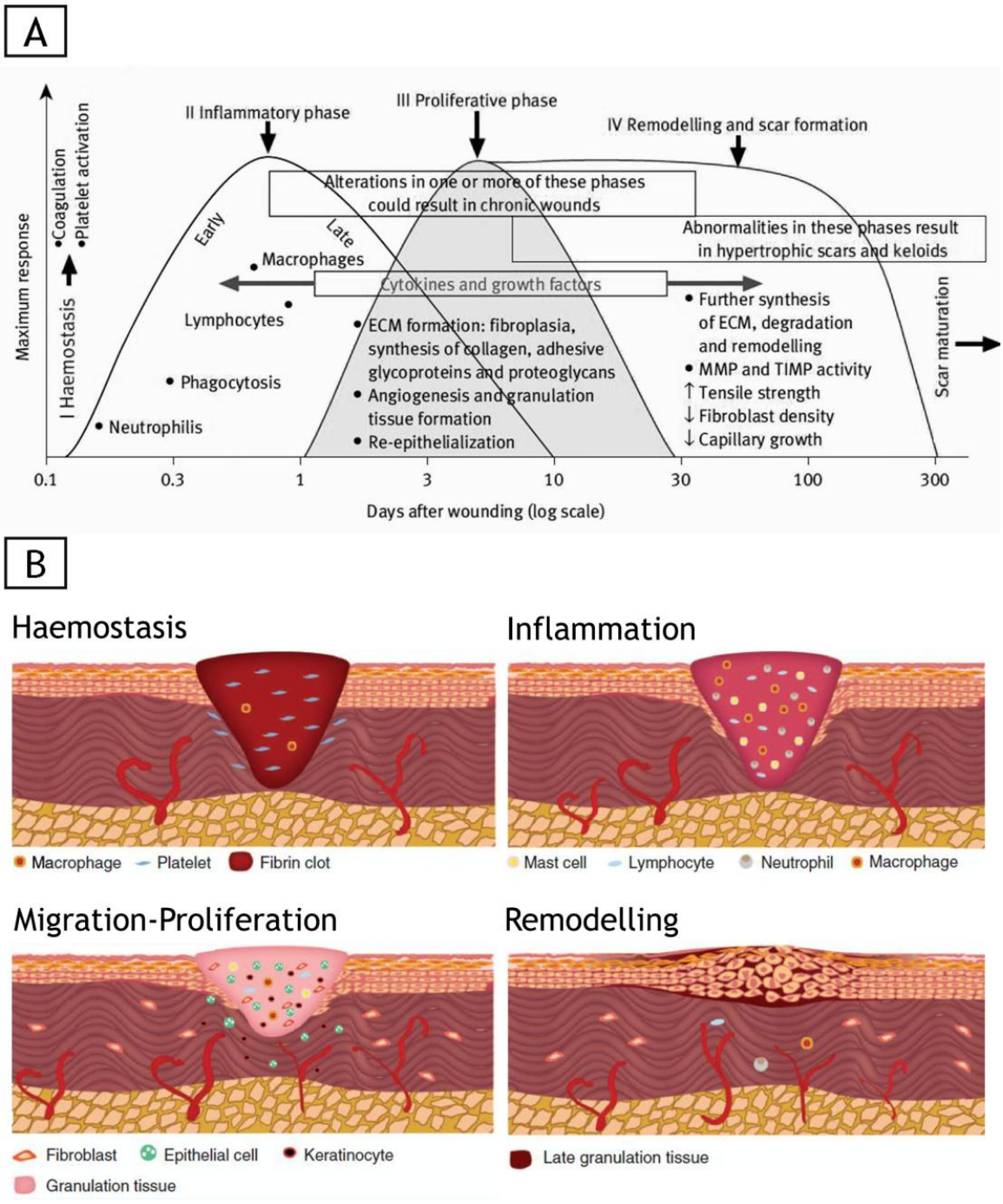

Figure 3: Schematic (A) and illustrative (B) representations of the main phases of the wound healing process. ECM: Extracellular matrix; MMP: Metalloproteinases; TIMP: Tissue inhibitors of metalloproteinases (adapted from [20, 26].

1.2.2.3. Cell migration and proliferation

The migration stage occurs 2-10 days after injury and begins the reestablishment of the wound. Epithelial cells and fibroblasts, from the edge of the wound, migrate into the injured local to restore the damaged and lost tissue. Almost simultaneously the proliferation phase starts (figure 3). In this phase, the wound is filled with granulation tissue. The endothelial cells of the adjacent venules initiate the angiogenesis process. These cells also synthesize remodelling enzymes that perform the breakdown of the ECM, creating defects into which new capillary vessels will grow and form a network, thus restoring the vasculature.

The migration of fibroblasts and ECM deposition are also characteristics of this stage. The fibroblast growth factor (FGF) and platelet-derived growth factor (PDGF) produced by macrophages attract fibroblasts into the wound site and some of them differentiate into myofibroblasts [16, 20, 21, 23, 24]. Once in the wound, fibroblasts and myofibroblasts interact, proliferate and produce matrix proteins like fibronectin, elastin, hyaluronan, collagen and proteoglycans. ECM is essential for cell adhesion and also for the regulation of cell growth, migration and differentiation within it. Moreover, fibroblasts also secrete FGF that along with vascular endothelial growth factor (VEGF), secreted by platelets and neutrophils, act as an angiogenic factor stimulating the endothelial cell proliferation and migration. Myofibroblasts are responsible for wound contraction, bringing the edges together.

The final stage of the proliferative phase is the epithelialization, where keratinocytes from the margin will proliferate and sustain wound epithelization [16, 20, 21, 23, 24].

1.2.2.4. Remodelling

Remodelling, also known as maturation, is the last step of wound healing (figure 3). It starts 2-3 weeks after injury and lasts for months to years. At this stage, all of the processes that were activated after injury cease, through the apoptosis of the majority of endothelial cells, macrophages and myofibroblasts leaving a mass that consists mostly of collagen and other ECM proteins. Metalloproteinases (MMPs) secreted by fibroblasts, macrophages and endothelial cells are continuously replacing collagen type III by mature collagen type I, allowing the constant remodelling of ECM. The initial granulation tissue is weak, but due to the collagen replacement, it becomes stronger. Sometimes, during the remodelling process an imbalance may occur and lead to abnormal scar formation [20, 23, 24].

1.3. Tissue engineering and skin substitutes

As previously described, skin damages can have different causes. One of the most common reasons for major skin loss are burns, specially thermal traumas [17]. The World Health Organization (WHO) estimates that each year over 300 000 people die from fire-related burn injuries and millions more suffer from physical and emotional consequences thereof [6].

The gold standard therapy used for burn wounds treatment and repair has been, and remains, the patients' own skin, known as Autograft [27]. In the case of severe burned patients, they lack sufficient adequate skin donor sites and so there is a clinical need for human cadaver skin, such as Allograft. Yet, the cadaver skin provides only temporary coverage, due to host immune rejection. Besides limited availability in skin banks, Allograft has other drawbacks, like variable quality, inconvenience of harvesting skin in the mortuary and the risk of disease transmission. Another approach used so far is Xenogeneic skin grafting or Xenograft, which involves the transfer of tissues between different species, but it has also rejection problems associated [10, 17, 28].

The demand for tissues and organs that can be used for regenerative purposes led to the appearance of tissue engineering. This interdisciplinary field applies the principles of engineering and life sciences toward the development of artificial tissues and its main purpose is to restore the function of damaged tissues or organs [29-31].

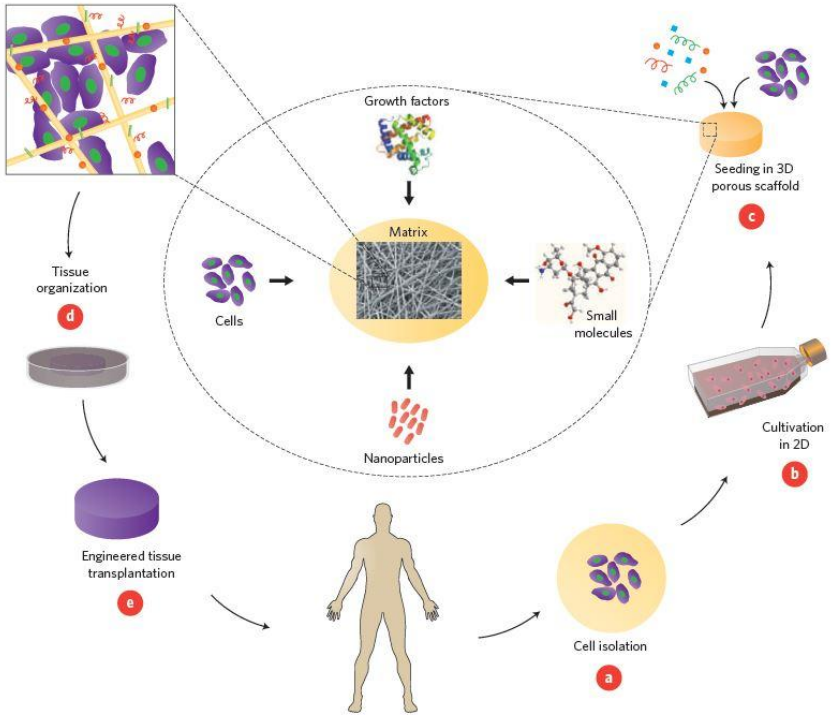

Figure 4: Representation of a tissue engineering model that involves seeding cells within a porous scaffold. a) Cells are isolated from the patient. b) *In vitro* cell culture on two-dimensional surfaces. c) Cells are seeded in a porous scaffold together with GFs, small molecules, and micro- and/or nanoparticles. The scaffold serves as a mechanical support and a shape-determining material, and it porous nature provides high mass transfer and waste removal. d) The cell construct is then cultivated in bioreactors to provide optimal conditions for it become a functioning tissue. e) Once the tissue has been successfully engineered, the construct is transplanted into the defect to restore tissue function (adapted from [30]).

The creation of tissue-engineered skin substitutes revolutionized the therapy of wounds that are not able to heal on their own (large - deep burns and chronic wounds) [3, 32]. The skin substitutes aim is to restore the structure and functions of native skin, in patients where these have been compromised [33].

Currently, different wound dressings and devices are available in the market, with new ones appearing each year. In the past, dressings like bandages, cotton wool, lint and gauze were used, being their primary function to keep the wound dry, allowing evaporation of exudates, and prevent the entry of harmful bacteria [16]. Nowadays it is well known that a warm moist wound environment is better than a dry one, since it achieves more rapid and successful the healing of the wound. Among the enormous list of wound dressings available, there isn't a single one that is able for the management of all wounds, since there are different types of

wounds (acute, chronic, epidermal, full-thickness, exuding and dry) and the healing process comprises various phases [16]. Therefore dressings can be classified in several ways, depending on their function in the wound (debridement, antibacterial, occlusive, absorbent and adhesive) [16], the type of the applied material (hydrocolloid, alginate, collagen) [34] and the physical form of the dressing (ointment, film, foam, gel) [35].

In the development of tissue-engineered materials it is necessary to take into account three major requirements: the safety of the patient, the clinical efficacy and the convenience of handling and application. In general, such biomaterials must be non toxic, do not induce immune response or cause excessive inflammation, and should also have a low risk of disease transmission [17, 33].

An ideal wound dressing should be able to play the role of ECM until host cells can repopulate a new natural matrix [36]. It should also maintain a moist environment, provide pain relief, protect the wound from infection, remove exudates, and be nonadherent to the wound in order to be removed without causing trauma [17, 37]. The biomaterial should be biodegradable and have similar mechanical and physical properties to the skin that it replaces. It is also of great interest the production of cost-effective skin substitutes, readily available, user-friendly and stored with a long-term storage [17].

According to Shakespeare [27] the functions that tissue-engineered skin products can offer are:

I. Protection — establishment of the mechanical barrier at the wound surface that restricts the access of microorganisms and also reduces fluid loss;

II. Procrastination — following early wound debridement, the cover of the wound is needed until its closure. For this purpose skin grafts and cultured autologous cells have been used in extensive burns;

III. Promotion— the delivery of dermal matrix components, cytokines and GFs to the wound bed can promote the wound healing process;

IV. Provision — supply new structures (dermal collagen or cultured cells) to be incorporated into the wound during healing process and persist thereafter.

The currently available skin substitute products are classified according to [17]:

- Anatomical structure that they are able to replace (epidermal, dermal, dermo-epidermal);
- Duration of the cover (temporary, permanent, semi-permanent);
- Type of biomaterial (biological or synthetic);
- Cellular component (cellular or acellular);
- Primary cellular loading of the biomaterial (*in vitro* or *in vivo*).

A key step in the design and production of **epidermal substitutes** is the isolation of keratinocytes from a donor. Cultured human keratinocytes (cultured epidermal autographs) were first used in 1981 for the treatment of extensive burns [17, 23]. The use of autologous keratinocytes is advantageous since the risk of rejection is very low. However, this kind of substitute presents some disadvantages, such as long culture time (about 3 weeks), difficulty to handle/apply and high production costs. To overcome the need to obtain a biopsy from each patient and then wait 2 to 3 weeks, epidermal cells from cadavers and adult donors have been used, despite the risk of rejection [3, 17, 28]. There are some approaches that make the keratinocytes handling and application easier, such as an aerosol of cell suspension (Cell Spray) and delivery membranes (MySkin) that can be made of synthetic materials (silicone) with a biological surface coating (collagen, fibrin glue, hyaluronic acid). Moreover, these delivery systems allow the reduction of culture and preparation times and thus an earlier clinical cell application. Other examples of some of the available epidermal substitutes are listed in table 1. These are being used to treat partial-thickness burns and chronic ulcers [17, 23].

Dermal substitutes (table 2) are usually acellular, based on allogeneic, xenogeneic or synthetic materials [38]. Dermal skin replacements present advantages, such as reduced costs, easier manufacture and rigorous quality control. They also add mechanical stability and prevent the wound from contracting [3, 17]. However, they can be rejected by the host and be involved in diseases transmission [8]. There are some dermal substitutes available, such as AlloDerm and Integra that are used to treat full- and partial-thickness wounds. Dermagraft, is applied for the treatment of full-thickness diabetic foot ulcers, Biobrane and Transcyte serve as temporary covering of partial-thickness burns and wounds [23].

Dermo-epidermal skin substitutes or composite skin substitutes (table 3) aim to mimic the native structure of skin (epidermal and dermal layers). These substitutes are more advanced and sophisticated than the epidermal and dermal ones, although they are the most expensive. Usually they are based on allogeneic skin cells incorporated into a dermal scaffold [17]. In

addition, Allograft, Apligraf and OrCel are examples of composite substitutes and can be used to treat burn wounds and venous and diabetic foot ulcers, respectively [23].

The selection of the scaffolding materials, with natural or synthetic origin, also plays an important role in the production of skin substitutes. Natural materials like chitosan, alginate, collagen, fibronectin, glycosaminoglycans (GAGs), hyaluronic acid (HA) and hydroxyapatite have a low toxicity level. The synthetic materials include polyglycolide, polylactide and polylactide coglycolide, among others [8].

Despite the different skin substitutes currently available, none of them can fully replace the functional and anatomical (layers, appendages, vascular and nerve network) properties of the native skin [17]. Still, significant progress has been made in the development of these products and in their clinical uses [3, 33].

Table 1: Examples of epidermal skin substitutes currently available in the market. Hyaluronic acid membrane (HAM); autologous (auto); recombinant (recomb); synthetic (synth); permanent (perm) [8, 17].

Product	Incorporated human cells	Primary cellular loading occurs	Cell source	Scaffold source	Scaffold material	Duration of the cover	Advantages	Drawbacks
Epicel	cultured keratinocytes	*in vitro*	auto	-	-	perm	large area of permanent wound coverage; little risk of rejection	3 weeks required to produce fragile confluent sheets; difficult to handle and apply; high cost
EpiDex	cultured keratinocytes from outer root sheath of scalp hair follicles	*in vitro*	auto	-	-	perm	cells have increased proliferative capacity and can be cryopreserved for repeat applications	takes up to 6 weeks after harvesting to produce; fragile product
MySkin	cultured keratinocytes	*in vitro*	auto	synth	silicone support layer with a surface coating	perm	more stable delivery platform; Keratinocytes can be thawed for repeated application	up to 14 days required for cell expansion; repeated application needed for good clinical outcome
Laserskin	cultured keratinocytes	*in vitro*	auto	recomb	HAM	perm	less fragile delivery system; improved mechanical stability	minimum of 3 weeks required to expand keratinocyte population
Cell Spray	non-/cultured keratinocytes	*in vitro*	auto	-	-	perm	more convenient way of delivering keratinocytes;	limited to partial-thickness and graft donor site wounds

Table 2: Examples of dermal skin substitutes currently available in the market. Polyglycolic acid (PGA); polylactic acid (PLA); extracellular matrix (ECM) derived from fibroblasts; glycosaminoglycans (GAGs); growth factors (GFs); allogeneic (allo); xenogeneic (xeno); synthetic (synth); permanent (perm); semi-permanent (semi-perm); temporary (temp) [8, 17].

Product	Incorporated human cells	Primary cellular loading occurs	Cell source	Scaffold source	Scaffold material	Duration of the cover	Advantages	Drawbacks
AlloDerm	-	in vivo	-	allo	human acellular freeze-dried dermis	perm	processing helps to reduce the antigenic components	risk of graft rejection and disease transfer
Integra	-	in vivo	-	xeno + synth	polysiloxane, bovine type I collagen, GAG	semi-perm	encourages ingrowth of fibroblasts and epithelial cells	antigenicity and disease risk; 3 weeks required to expand the dermal autograft
Dermagraft	cultured neonatal fibroblasts	in vitro	allo	allo + synth	PGA/PLA, ECM	temp	neonatal fibroblast rapidly proliferate to produce collagen, GAGs and GFs	risk of rejection and disease risk
TransCyte	cultured neonatal fibroblasts	in vitro	allo	xeno + synth	silicon film, nylon mesh, porcine dermal collagen	temp	dermal fibroblasts secrete collagen, GAGs and GFs	non degradable; risk of being rejected by the host and disease transmission
Biobrane	-	in vivo	-	xeno + synth	silicon film, nylon fabric, porcine collagen	temp	reduces pain; provide matrix proteins and GFs	non degradable; rejection and disease risk

Table 3: Examples of dermo-epidermal skin substitutes currently available in the market. Growth factors (GFs); allogeneic (allo); xenogeneic (xeno); temporary (temp) [8, 17].

Product	Incorporated human cells	Primary cellular loading occurs	Cell source	Scaffold source	Scaffold material	Duration of the cover	Advantages	Drawbacks
Allograft	native	native	allo	allo	Cadaveric human skin with dermal and epidermal cells	temp	can be used either fresh or frozen; sterilization techniques reduce the risk of infection	risk of rejection and disease; limited availability
Apligraf	cultured keratinocytes and fibroblasts	*in vitro*	allo	xeno	bovine collagen	temp	improves granulation tissue deposition; no signs of rejection from the host	risk of chronic graft rejection and disease; requires repeated applications
OrCel	cultured keratinocytes and fibroblasts	*in vitro*	allo	xeno	bovine collagen sponge	temp	favourable environment for host cell migration; source of cytokines and GFs	risk of rejection and disease

1.4. Hydrogels

Hydrogels are insoluble three-dimensional (3D) networks of crosslinked hydrophilic polymers that are promising to be used in tissue engineering applications [39]. Hydrogels own the most desirable characteristics of an "ideal dressing", like biocompatibility and biodegradability, structural similarity to ECM, permeability and water uptake capacity. Hydrogels are able to maintain a moist environment that is crucial for improving the wound-healing process, by preventing tissue dehydration, as well as the capacity to absorb tissue exudates, avoiding fluid accumulation that could lead to skin maceration and microbial proliferation. The moist environment will also encourage rapid granulation tissue formation and re-epithelialization [16, 36]. In addition, hydrogels are highly permeable to gases, like oxygen that will help in angiogenesis, nutrients and waste products [40]. The biocompatibility and biomimetic microstructure of hydrogel, resembling natural tissues, provides a 3D structure for cell adhesion and proliferation [36]. However, hydrogels present some drawbacks related to sterilization issues and low mechanical strength, being too soft and weak to be applied in some tissue engineering applications [41].

A significant progress has been made in the design and synthesis of hydrogels, allowing their use in several biomedical applications such as wound dressings, drug delivery vehicles (antibiotics and GFs), cell based therapies and anti-adhesion materials [39, 42-44]. Furthermore, the ability of hydrogels to be formed *in situ* and administered through a minimally invasive procedure (injectable system) extends its range of applications. Depending on the pretended application, the materials used for the production of hydrogels must be different and subsequently their properties will also be varied [44-46].

Hydrogels can be classified into different categories depending on their macromolecular precursors and the synthesis process used for their manufacture. They can be produced with natural and synthetic sources [42, 47]. Natural polymers include alginate, chitosan, chondroitin sulphate, collagen, elastin, fibrin, gelatine, heparin and HA. These polymers have attracted a lot of attention for biological applications due to their resemblance to the ECM components, high chemical versatility and biodegradability. However, they present some disadvantages such as low mechanical properties and inability to control their degradation and structure. On the other hand, synthetic polymers like poly(ethylene glycol) (PEG), poly(ethylene oxide) (PEO), poly(vinyl alcohol) (PVA), poly(2-hydroxyethyl methacrylate) (PHEMA), and polyacrylamide (PAM), generally show high mechanical properties, but lack biological moieties. Due to the natural and synthetic polymers' characteristics, they can be blended in order to create hydrogels with unique properties for biomedical and biotechnological applications [39, 47].

These polymers can be physically or chemically crosslinked to produce polymeric networks and preserve their 3D structures [42, 47]. Physical crosslinking is achieved through the formation of physical bonds between the polymer chains. Physically crosslinked hydrogels are formed through changes in environmental conditions (pH, temperature and ionic interactions), hydrogen bonds and protein interactions, without the need of chemical crosslinkers. *In situ* forming physical hydrogels, after injection, instantaneously change from sol to gel state under physiological temperature and pH conditions. However, they present low mechanical properties, which limit their application in the area of tissue engineering. On the other hand, chemical crosslinking creates stable covalent bonds between the polymers chains. Chemically crosslinked gels can be obtained by radical polymerization, chemical reactions, energy irradiation and enzymatic crosslinking. *In situ* forming chemical hydrogels can have their mechanical properties adjusted by the degree of crosslinking. Despite the improved mechanical properties, these hydrogels can have some cytotoxicity due to the presence of some residues of the crosslinkers [39, 41, 45, 48].

The physical, chemical and biological properties of hydrogels can be modulated by varying the combination of materials and the degree of crosslinking, resulting in a series of biomaterials with specific mechanical and functional requirements that satisfy the demands of a target tissue [49].

1.4.1. Photocrosslinkable Hydrogels

Recently photocrosslinkable hydrogels have attracted a lot of attention for many biomedical applications, like tissue engineering scaffolds, drug delivery and cell therapy. This increased interest is due to *in situ* delivery of polymeric solutions containing cells and/or bioactive molecules with a minimally invasive method and fast crosslinking under brief exposure to UV or visible light [43, 50, 51]. The use of light to cure materials *in vivo* has been used extensively in dentistry to form sealant and dental restorations. Photopolymerization has also been used for other applications, such as membranes, blood vessel adhesives, coatings, and for encapsulation of pancreatic islet cells [40, 52].

Photocrosslinkable hydrogels are covalently crosslinked by exposing a precursor photocurable polymer solution to light, in the presence of a non-toxic photoinitiator (PI) [51]. The UV light is the most commonly used to induce the photoinitiator to generate free radicals. These free radicals subsequently attack the alkene groups of the precursor polymer, creating covalent bonds that crosslink the hydrogel network [47]. Photocrosslinkable hydrogels offer some

advantages over other types of crosslinking methods like biocompatibility, *in situ* forming at physiological temperature and pH, fast curing rates, temporal/spatial control and low cost. However, they present some drawbacks such as the production of free radicals during the crosslinking reaction that may lead to DNA damage and the limited light penetration through tissues [40, 41, 47, 53].

Synthetic (PEG and PHEMA) and natural (alginate, chitosan, collagen, dextran, gelatine, HA) polymers have been modified with photocrosslinkable functional groups, like methacrylate groups, to yield photocurable gels [39, 47]. Since unreacted monomers from synthetic polymers can be toxic, natural polymers have receiving an increasing attention [54].

Furthermore, the choice of the more appropriated PI, light intensity and exposure time are critical for limiting possible deleterious effects on cells and bioactive molecules, and also control hydrogels mechanical properties [43, 55, 56]. Bryant and colleagues investigated the viability of NIH-3T3 cells (mouse embryonic fibroblasts) where different PIs were used and concluded that one in particular, 2-hydroxy-1-[4-(hydroxyethoxy)phenyl]-2-methyl-1-propanone (Irgacure 2959), displayed a minimal toxicity for cell encapsulation in hydrogels [57]. Williams et al. evaluated the toxicity profiles of some PIs on six different cells lines (bovine chondrocytes, goat bone marrow-derived mesenchymal stem cells, human bone marrow-derived mesenchymal stem cells, rabbit corneal epithelial cells, human fetal osteoblasts and human embryonic germ cells). Their study also revealed that the photoinitiator Irgacure 2959, was cytocompatible for the tested cells [52].

In vivo, the formation of photopolymerized hydrogels can be performed using bulk or interfacial photopolymerization. The most commonly used is bulk photopolymerization, where the PI is dissolved in the precursor polymer solution and under exposure to light, the precursor solution is converted to a hydrogel. In interfacial photopolymerization, the PI is adsorbed onto the surface of tissues/cells and then the hydrogel precursor solution is added. The subsequently exposition to light allows the creation of thin hydrogel linings on the surface of tissues/cells [40]. Moreover, photopolymerization through transdermal illumination is a promising way to induce polymerization of hydrogels that are injected subcutaneously without large incisions (using laparoscopic devices, catheters or subcutaneous injection). Furthermore this also improves the intimate contact of the polymer with the surface of the tissue at the implantation site [39-41, 58, 59].

Ishihara et al. evaluated a photopolymerizable chitosan hydrogel as a dressing for wound occlusion to improve the healing process, using a mouse model with full thickness-skin incisions. The study revealed that the photocrosslinkable chitosan hydrogel is a promising dressing for wound occlusion and for being used as a tissue adhesive, especially suitable for

situations where urgent haemostasis is required [60]. Fujita and colleagues developed a photocrosslinkable chitosan hydrogel containing FGF-2, as a myocardial angiogenic therapy using a rabbit model of myocardial defect. The results indicated that the FGF-2/chitosan hydrogel efficiently induces angiogenesis and collateral circulation and protects the myocardium, thus suggesting a potential therapeutic value, especially to diffuse myocardial ischemia or residual ischemic lesion in surgical bypass [61].

1.5. Chitosan

Chitosan is a natural polysaccharide composed of glucosamine and N-acetyl-glucosamine (figure 5). It was produced for the first time in 1859 by Rouget and colleagues through the deacetylation of chitin [62]. Chitin is the second most abundant polysaccharide in nature, being found in the shells of crustaceans, exoskeleton of insects and cell walls of fungi [63-65].

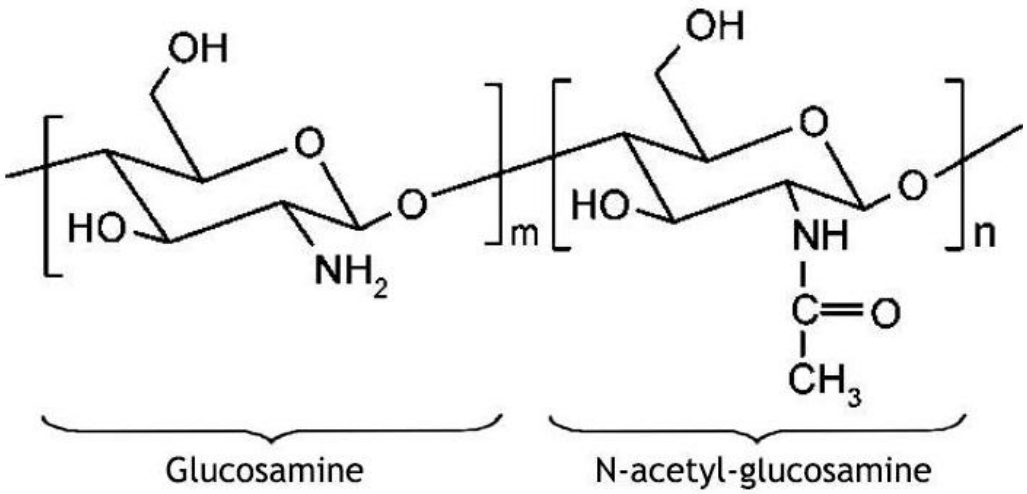

Figure 5: Representation of chitosan structure (adapted from [66]).

The deacetylation degree (DD) of commercial chitosan is usually between 70% and 95%. The different degrees of deacetylation are defined in terms of the percentage of primary amine groups in the polymer backbone [64]. Chitosan with higher DD presents a greater number of free amino groups. This allows the interaction between chitosan and cells, stimulating their adhesion and proliferation and also improves its antimicrobial and haemostatic activities, thus enhancing tissue regeneration [67].

Chitosan is gradually degraded *in vivo*, by certain human enzymes, especially lysozyme, releasing N-acetyl-glucosamine, which initiates fibroblasts proliferation, stimulates HA and type IV collagen synthesis at the wound site. Thus, improving wound healing and also scar prevention [36, 67, 68].

A disadvantage of this polymer is its pH-sensitive behaviour, due to the large quantities of amine groups on its chain, chitosan dissolves easily at low pH and it is insoluble in basic solutions. However, as chitosan consists of both reactive amine and hydroxyl groups, it can be chemically and physically modified, increasing its versatility [64, 69].

Furthermore, due to its low cost and availability, biocompatibility, biodegradability and bioadhesive properties, chitosan has attracted great attention for the tissue engineering field. Chitosan has been used to produce hydrogels, scaffolds, sponges, membranes, nanofibers, beads, microparticles and nanoparticles, to be applied for different biomedical applications in skin, bone, cartilage and vascular grafts [64, 68, 70].

1.6. Gelatine

Gelatine is a natural polymer (figure 6) derived from collagen, which is the most abundant protein in skin, bone, cartilage and tendons.

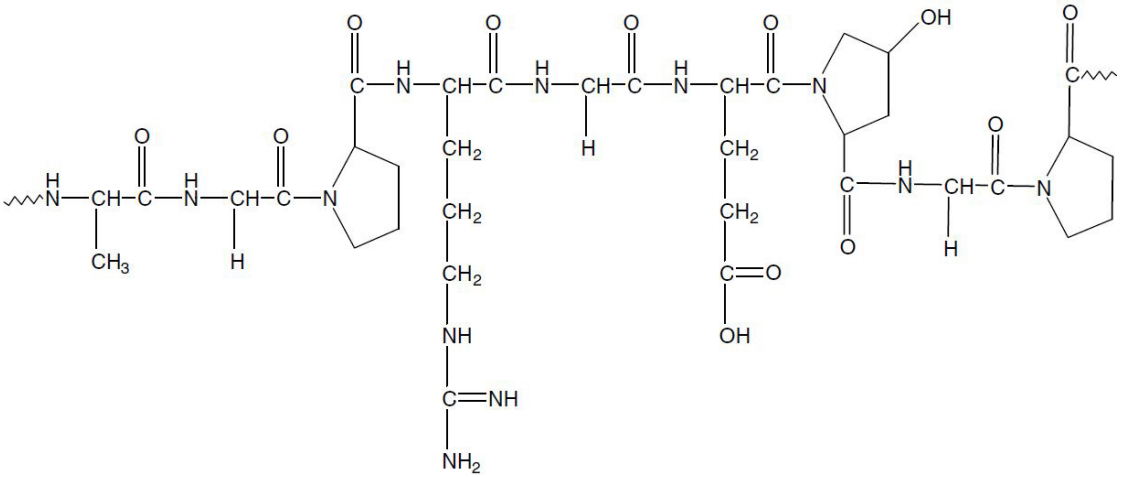

Figure 6: Representation of gelatine structure (adapted from [71]).

This polymer has several advantages, such as low cost and low immunogenicity. It is soluble at 40°C and at physiological pH. Moreover, gelatine is biocompatible and biodegradable (by collagenases). The large number of amine, carboxyl and hydroxyl groups, allows gelatine

chemical modification and increases its versatility [72]. Moreover, gelatine contains Arg-Gly-Asp (RGD)-like sequences that promote cell adhesion, proliferation and migration [63, 72, 73].

Gelatine has widespread applications in food (emulsifiers, foaming agents, colloid stabilizers, fining agents, biodegradable packaging materials and micro-encapsulating agents), cosmetic and pharmaceutical industry, specially due to its gel-forming properties [74]. Since 1970, gelatine has also being used in the tissue engineering field to produce scaffolds and wound dressings for both soft and hard tissue engineering [36, 75].

Two relevant gelatine products, commercially available are Gelfilm, an absorbable film for use in thoracic, ophthalmic and neuro-surgery, and Gelfoam, a compressed gelatine sponge that is used as a haemostatic device. Recently, gelatine scaffolds, specially the photocrosslinkable ones, have been used in several tissue engineering applications such as cartilage repair, blood vessels generation and cardiac tissue development [76].

1.7. Aims

The overall aim of the present thesis was to design and develop new photopolymerizable hydrogels based on natural polymers, to be used as skin substitutes. The specific aims of this study were:

- Modification and characterization of chitosan and gelatine;
- Development of chitosan-gelatine photopolymerizable hydrogels;
- Evaluation and characterization of the physicochemical properties of the produced hydrogels;
- Characterization of roughness and porosity of the developed hydrogels through scan electron microscopy analysis;
- Evaluation and characterization of the biological properties of the produced hydrogels;

Chapter II

Materials and Methods

2. Materials and Methods

2.1. Materials

Antibiotic-antimycotic (penicillin and streptomycin), Bovine serum albumin (BSA), Chitosan (medium molecular weight (MMW) 190.000-310.000 $g.mol^{-1}$), Cellulose dialysis membrane, Dulbecco's modified Eagle's medium (DMEM-F12), Ethylenediaminetetraacetic acid (EDTA), Gelatine, Glutaraldehyde, Irgacure 2959, Methacrylic anhydride (MA), Phosphate-buffered saline solution (PBS), Trypan blue and Trypsin were purchased from Sigma-Aldrich (Sintra, Portugal). Acetic acid and Sodium hydroxide were acquired from Pronalab (Barcelona, Spain). Normal Human Dermal Fibroblasts (NHDF) were bought from PromoCell (Labclinics, S.A.; Barcelona, Spain). Fetal bovine serum (FBS) was obtained from Biochrom AG (Berlin, Germany). 3-(4,5-dimethylthiazol-2-yl)-5-(3-carboxymethoxyphenyl)-2-(4-sulfophenyl)-2H-tetrazolium (MTS) was purchased from Promega (Canada, USA). Tris Base was purchased from Fisher Scientific (Portugal).

2.2. Methods

2.2.1. Synthesis and characterization of deacetylated Chitosan

The deacetylation of chitosan was performed through a method previously described in the literature [77]. Briefly, 500 mg of MMW chitosan were mixed with 10 ml of 1 M NaOH. The mixture was heated at 50°C, under magnetic stirring, for 3 h and then filtered with a 0.44 μm filter and a Buchner funnel. The remaining material was washed extensively with ultrapure water until a neutral pH was obtained. The samples were then dried at 40°C overnight.

In order to determine the DD, the recovered chitosan was dissolved in 1 M acetic acid, filtered with a 0.22 μm filter to remove any solid particles. Subsequently, the pH was adjusted to 7 with 1 M NaOH, resulting in chitosan precipitation. The product was then centrifuged three times at 4500 rpm (Sigma 3K18C centrifuge) and finally the recovered pellet was freeze-dried (Scanvac CoolSafe™, ScanLaf A/S, Denmark) for 24 h. The DD was measured by a first derivative UV-spectroscopy (1DUVS) method [78].

2.2.2. Synthesis of methacrylamide chitosan

Methacrylamide chitosan (MAC) was synthesized using a method previously described in the literature with slight modifications [79]. Briefly, the deacetilated chitosan was dissolved 3% (wt/v) in acetic acid overnight. After complete dissolution, the MA was added dropwise and allowed to react for 4 h. The mixture was then dialyzed against ultrapure water using dialysis tube (molecular weight cutoff: 12-14 KDa), for 5 days at room temperature (RT), to remove unreacted MA and additional water soluble contaminants. The water was changed three times per day. Finally, the solution was freeze-dried to obtain pure MAC and stored at -80°C, until further use.

2.2.3. Synthesis of methacrylamide gelatine

Similarly, methacrylamide gelatine (MAG) was synthesized as previously described in the literature with slight modifications [41]. Briefly, gelatine was dissolved 10% (wt/v) in ultrapure water, at 40°C. After gelatine was completely dissolved, MA was added dropwise, with vigorous stirring. The methacrylation reaction took 1 h and the resultant solution was afterwards dialyzed against ultrapure water in 12–14 kDa cut-off dialysis tube, for 5 days at 40°C, to remove unreacted MA and additional water soluble contaminants. The water was changed three times per day. Finally, the solution was freeze-dried to obtain pure MAG and stored at -80°C, until further use.

2.2.4. Nuclear Magnetic Resonance

The degree of methacrylation (DM) of MAC and MAG polymers were quantified by proton Nuclear Magnetic Ressonance (^{1}H NMR) spectroscopy, by using a Brüker Advance III 400 MHz spectrometer (Brüker Scientific Inc., USA). Prior to spectra acquisition, chitosan and MAC were dissolved in 1 mL of deuterium chloride (DCl) and deuterium oxide (D_2O) at RT, and gelatine and MAG were dissolved in 1mL of D_2O, at 40°C. Then samples were carefully transferred to 5 mm NMR glass tubes. All the ^{1}H spectra were acquired at a constant temperature of 25°C, using pre-saturation for water suppression. The data was recorded with a spectral width of 0 to 7.5 kHz. Then, the recorded spectra were processed and integrated with the TOPSPIN 3.1 software (Brüker Scientific Inc). The DM was calculated from the integration of the appropriate peaks [79, 80].

2.2.5. Hydrogel production

Initially a MAC stock precursor solution of 2% (wt/v) was prepared by dissolving the freeze-dried MAC polymer in ultrapure water containing 0.25% (wt/v) of PI Irgacure 2959. Likewise, a MAG stock precursor solution of 20% (wt/v) was prepared by dissolving the freeze-dried MAG polymer in ultrapure water containing 0.25% (wt/v) of PI Irgacure 2959. MAC:MAG precursor solutions were also prepared using different volume ratios, 2:1, 1:1 and 1:2, of MAC and MAG stock solutions.

Table 4: Volumes of MAC and MAG stock precursor solutions (containing Irgacure 2959 0.25% (wt/v)) used for the preparation of hydrogels precursor solutions.

Hydrogels precursor solutions	MAC stock precursor solution 2% (wt/v)	MAG stock precursor solution 20% (wt/v)
MAC	12 mL	-
2:1	8 mL	4 mL
1:1	6 mL	6 mL
1:2	4 mL	8 mL
MAG	-	12 mL

To fabricated MAC, MAG and MAC:MAG hydrogels, 100 µL of the previously prepared "hydrogels precursor solutions" (see table 5) were pipetted into a silicon mould and subsequently exposed to UV light, 254 nm, ~7 mW/cm^2 (UVC 500 Ultraviolet Crosslinker) for 20 and 10 min, respectively.

2.2.6. Fourier transform infrared spectroscopy analysis

Fourier transform infrared spectroscopy is extensively applied for identifying the chemical structure of hydrogels by comparing the materials used in their production. In this technique, the chemical bonds can be excited and absorb the infrared light at characteristic frequencies. The resulting spectra represent the frequencies that are characteristics of each type of

chemical bond [81]. FTIR analysis of MAC and MAG polymers, and MAC:MAG freeze-dried hydrogels was performed. The FTIR spectra were acquired in a Nicolet iS10 spectrometer (Thermo Scientific Inc., USA) equipped with a Smart iTR auxiliary, by recording 256 scans with a spectral width from 500 - 4000 cm^{-1}, at a spectral resolution of 4 cm^{-1}.

2.2.7. Water uptake capacity of the hydrogels (Swelling)

The swelling properties of MAC:MAG hydrogels were assessed in Tris buffer (pH 5) solution. After being produced, the hydrogels were lyophilized and weighted. The dry hydrogels (n=3) were placed in eppendorfs with 1 mL of the swelling solution at 37°C, under constant shaking (60 rpm). At predetermined time intervals the hydrogels were bottled out, gently wiped with filter paper, to remove the excess of liquid in the samples surface, weighted and re-immersed in the solution. The process was repeated until the hydrogels reached equilibrium [55]. The swelling ratios were evaluated through equation (1):

$$Swelling\ ratio\ (\%) = \frac{Ws - Wd}{Wd} \times 100 \qquad (1)$$

Where W_d is the initial weight of dry hydrogel and W_s is the weight of swollen hydrogel.

2.2.8. Porosity evaluation

The total porosity of the MAC:MAG hydrogels was determined by adapting a displacement method previously reported [82]. The porosity of the lyophilized hydrogels was determined, after 24 h of immersion in ethanol, using the following equation (2):

$$Porosity\ (\%) = \frac{Ws - Wd}{d\ ethanol\ \times V\ hydrogel} \times 100 \qquad (2)$$

Where W_d is the initial weight of dry hydrogel and W_s is the weight of swollen hydrogel, $d_{ethanol}$ the density of the ethanol at RTand $V_{hydrogel}$ is the volume of the swollen hydrogel. For each hydrogel, three replicates were analyzed and the data represent the average of each replicate.

2.2.9. Characterization of the cytotoxic profile of the hydrogels

NHDF cells were seeded in T-flasks of 25 cm^2 with 6 mL of DMEM-F12 supplemented with heat-inactivated FBS (10% v/v) and 1% antibiotic/antimycotic solution. When the confluence was achieved, they were sub-cultivated by 3-5 minutes incubation in 0.18% trypsin (1:250) and 5 mM EDTA. Then cells were centrifuged, resuspended in culture medium and then seeded in T-flasks of 75 cm^2. Hereafter, cells were kept in culture at 37°C in a 5% CO_2 humidified atmosphere, inside an incubator [18, 83].

In order to assess the cytotoxicity of the hydrogels, each crosslinked hydrogel was taken out of the cast and cut into the desired shape. The materials were sterilized by immersion in ethanol 70% for 30 min and afterwards washed with sterile PBS for 15 minutes, three times [72, 84]. Then, the hydrogels (n=5) were placed into a 96-well flat bottom culture plate. NHDF cells were seeded in wells containing the sterilized hydrogels at a density of $2x10^4$ cells per well and incubated at 37°C in a 5% CO_2 humidified atmosphere, for 24 and 72 h. Subsequently, an MTS assay was performed. Briefly, the culture medium of each well was removed and replaced with a mixture of 100 µL of fresh medium and 20 µL of MTS reagent solution and then the cells were incubated for 4 h, at 37°C, under a 5% CO_2 humidified atmosphere. Afterward, cell viability was assessed through the reduction of the MTS into formazan. The absorbance of the produced formazan was measured at 492 nm using a microplate reader (Sanofi, Diagnostics Pauster). Ethanol 96% was added to cells as a positive control (k^+) while cells without materials were used as a negative control (k^-) [22].

2.2.10. Proliferation of fibroblast cells in the presence of the hydrogels

MAC, MAG and MAC:MAG hydrogels were produced and sterilized using ethanol, as previously described [84]. To evaluate cell behaviour in the presence of the hydrogels herein produced, the materials (n=5) were placed into a 96-well flat bottom culture plate. NHDF cells were seeded in wells containing the sterilized hydrogels at a density of $2x10^4$ cells per well and incubated at 37°C in a 5% CO_2 humidified atmosphere, for 24 and 72 h. Cell growth was monitored using an Olympus CX41 inverted light microscope (Tokyo, Japan) equipped with an Olympus SP-500 UZ digital camera [18, 83]. NHDF cells were then seeded on hydrogels surface at a density of $2x10^4$ cells per well and incubated at 37°C, under a 5% CO_2 humidified atmosphere.

2.2.11. Scanning electron microscopy analysis

Scanning electron microscopy (SEM) was used to characterize the morphology of the MAC:MAG hydrogels. A sample of each hydrogel was frozen in liquid nitrogen and fractured to expose the cross-section. The average pore size of the MAC:MAG hydrogels was determined using ImageJ software (National Institutes of Health, Bethesda (MD), USA). Fibroblast cells adhesion and morphology, after 24 and 72 h, on the surface of the MAC:MAG hydrogels were also characterized. The hydrogels with cells were fixed overnight with 2.5% glutaraldehyde in PBS, at 4°C. Samples were rinsed with PBS and dehydrated in graded ethanol of 70, 80, 90 and 100%, 10 min each. All the samples with/without cells were subsequently freeze-dried and mounted on an aluminium board using a double-sided adhesive tape and sputter coated with gold using a Q150R ES (United Kingdom) sputter coater. The samples were analyzed using a Hitachi S-3400N (Tokyo, Japan) scanning electron microscope operated at an acceleration voltage of 20 kV, at various magnifications [22, 85].

2.2.12. Statistical analysis of the results

Statistical analysis of the obtained results was performed using one-way ANOVA with Dunnet´s post hoc test and Newman-Keuls multiple comparison test (***, ###, §§§ $p<0.001$). Each result is the mean ± standard error of the mean of at least three independent experiments.

Chapter III

Results and Discussion

3. Results and Discussion

3.1. Characterization of photocrosslinkable chitosan

The degree of deacetylation of chitosan is defined as the percentage of primary amine groups available on the chitosan backbone. Chitosan DD is an important factor that determines several physiochemical and biological properties such as hydrophilicity, degradation and cell response. Moreover, chitosan amine groups promote cell proliferation [83]. The increase of amine groups in the chitosan chain, through deacetylation, was necessary for the synthesis of a photo-curable chitosan, MAC, while maintaining the chitosan properties [66].

Chitosan DD can be controlled by processing the polymer with an alkaline treatment that include high temperatures [86]. The higher the chitosan DD, the greater the number of free amine groups. In this study the DD of the deacetilated chitosan was approximately 95%.

Table 5: Degree of deacetylation of the commercial MMW chitosan and the produced deacetilated chitosan (mean ± SD, n=3). The nominal DD was provided by the manufacturer. The DDs were determined by 1DUVS.

Sample	Nominal DD (%)	Determined DD (%)
Commercial MMW Chitosan	75 - 85	83.4 ± 0.2
Deacetilated Chitosan	-	95.1 ± 0.5

The polymers functionalization was performed with methacrylic anhydride, due do its alkene groups that will be attacked by free radicals (benzoyl and ketyl radicals), generated by the PI when exposed to UV light, forming covalent bonds that render high stability to the polymers network [39, 40]. After the synthesis of MAC, its degree of methacrylation was determined through NMR analysis. The ^{1}H NMR spectra obtained for the deacetilated chitosan and MAC are shown in figure 7. In comparison with the NMR spectrum of chitosan (figure 7 A), it can be observed that the spectrum of MAC presents the characteristic peaks of chitosan. An assignment of the proton peaks, obtained in the NMR spectra, was performed according to the chemical shift previously reported in the literature [55, 79, 87]. As can be observed in figure 7 A and B, the proton peak appearing at 1.9 ppm corresponds to $-CH_3$, of the acetyl group

from N-acetyl-glucosamine residue and the peak at 3.1 ppm is attributed to the proton H2 of glucosamine residue. Furthermore, the peaks at 3.4-3.9 ppm are assigned to the protons H3-H6 of chitosan [55, 79, 87]. The incorporation of the methacrylic anhydride double bonds (-C=CH_2) and –CH_3 groups into chitosan was confirmed by the appearance of the proton peaks at 5.6, 6.0 and 1.7-1.9 ppm, respectively (figure 7 B) [66, 87].

The DM of the chitosan was defined as the percentage (%) of amine groups (-NH_2) substituted with methacrylate groups. DM was calculated based on the ratio of the integrated area of the proton peaks H2-H6 at 2.8-3.9 ppm to that of methylene peaks at 5.5-6.1 ppm, and revealed to be approximately 33% [79].

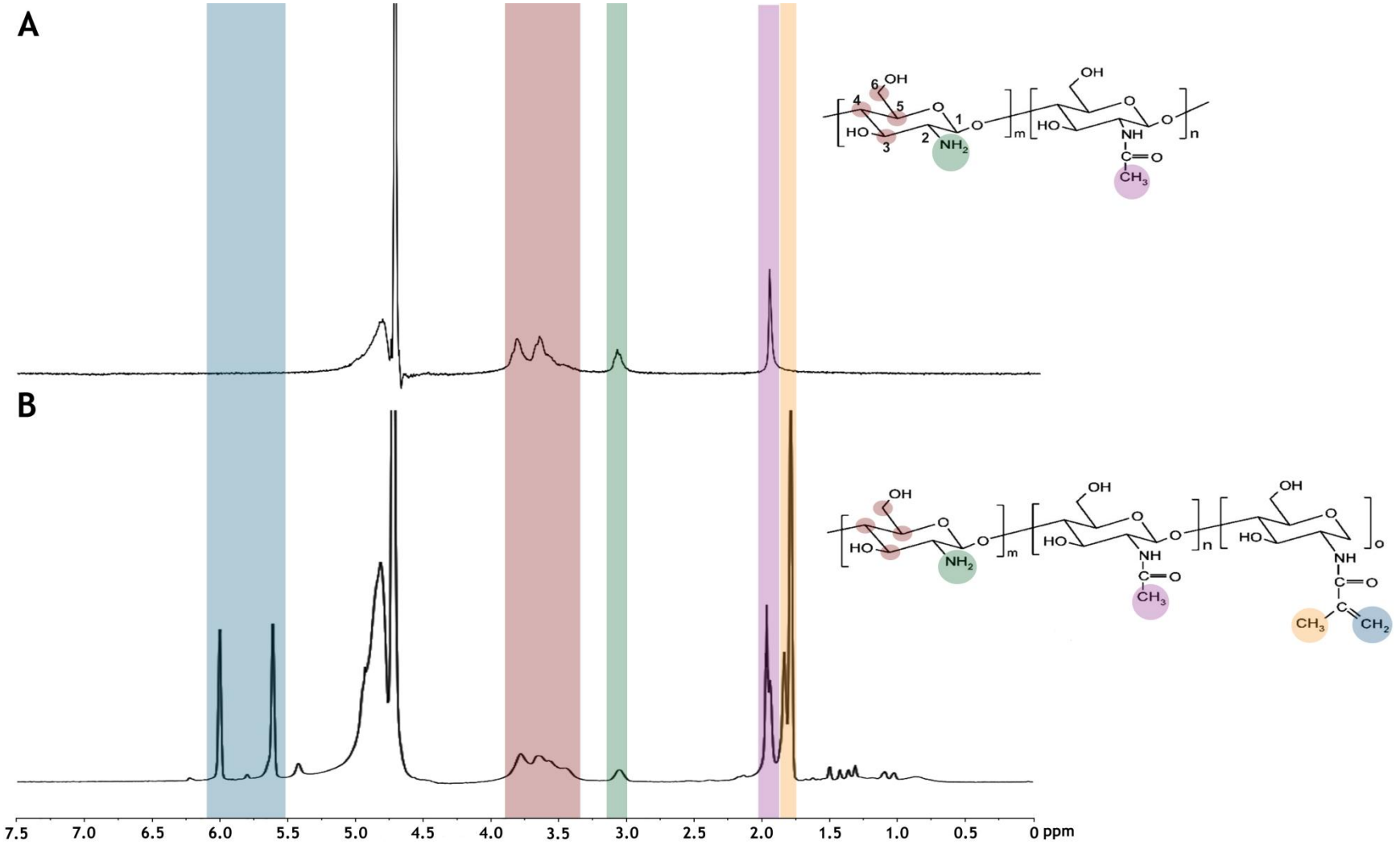

Figure 7: ^{1}H NMR spectra of deacetilated chitosan (A) and methacrylamide chitosan (B).

3.2. Characterization of photocrosslinkable gelatine

For the synthesis of the photocrosslinkable gelatine, MAG, the primary amine groups of gelatine, were also modified with methacrylic anhydride [66]. To evaluate the success of the synthesis process and determine the DM of MAG, an NMR analysis was performed.

The ^{1}H NMR spectra obtained for unmodified gelatine and MAG are shown in figure 8. The assignment of the proton peaks presented in the NMR spectra, was performed according to the chemical shift previously reported in the literature [41, 72, 80, 88]. Comparing the NMR spectra of gelatine and MAG it can be observed the spectrum of MAG (figure 8 B) presents the characteristic peaks of gelatine (figure 8 A). The proton peak appearing at 7.1-7.4 ppm corresponds to the phenylalanine (aromatic residues) signal. In addition, the peak at 2.8-3.0 ppm is assigned to the lysine methylene signals [41, 72, 80, 88] Moreover, new peaks can be observed at 5.4 and 5.6 ppm (figure 8 B), which confirms the incorporation of the methacrylic anhydride double bonds (-C=CH_2) and –CH_3 groups into the gelatine chain [41, 72, 80, 88].

The DM of MAG was defined as percentage of gelatine amine groups functionalized with methacrylate groups. The DM was calculated based on the ratio of the integrated area of the lysine methylene signals (2.8-3.0 ppm) of the MAG and unmodified gelatine spectra, and revealed to be approximately 23% [72, 80]. Some minor reactions might have occurred with other reactive groups, like hydroxyl groups [80].

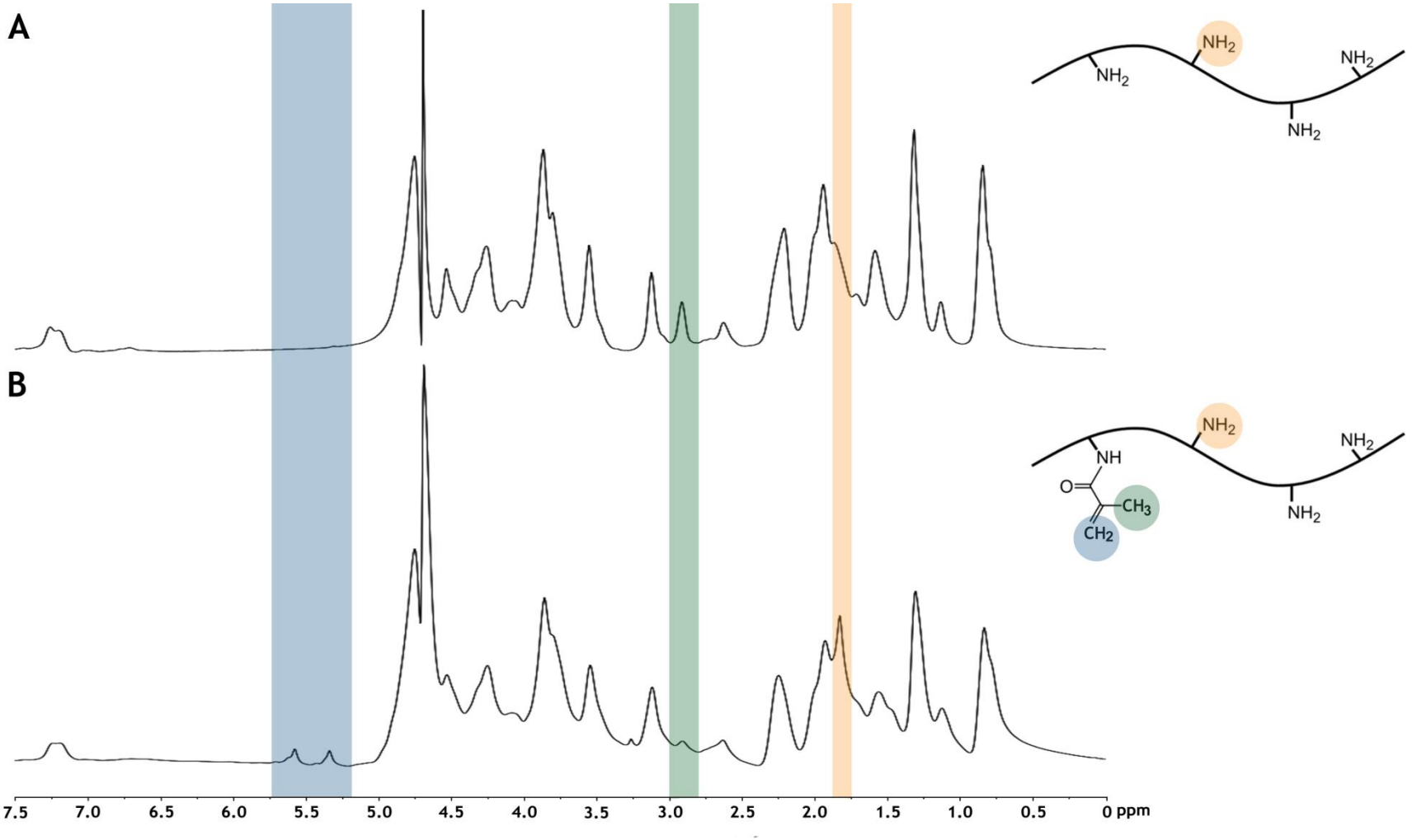

Figure 8: ^{1}H NMR spectra ofunmodified gelatine (A) and methacrylamide gelatine (B).

3.3. Hydrogel production and morphology characterization

Hydrogels have been extensively used so far due to their capacity to mimic the ECM and thus provide a suitable environment for cells adhesion, proliferation and maintenance [85]. Due to the advantages of photocrosslinkable hydrogels, they have attracted a huge attention from researchers [41, 47, 53]. Herein, chitosan and gelatine photocrosslinkable hydrogels were produced.

When tissue engineering applications are envisioned, the solubility of chitosan at physiological pH is important because it allows the encapsulation of cells and pH-sensitive proteins [79]. Usually chitosan is only soluble in dilute acid, however the modification of some chitosan amine groups with methacrylic anhydride yielded a water-soluble chitosan [79, 89]. Yu *et al*. reported the preparation of a methacrylamide chitosan scaffold for neural tissue engineering applications. However, they used ammonium persulfate (APS) and sodium metabisulfite (SMBS) as initiators, which can be cytotoxic to cells and host tissues [79]. Moreover, this methacrylamide chitosan, even with a low degree of methacrylation, required a much longer gelation reaction time, 2 h, compared with the 20 min necessary for the gelation of the MAC hydrogel produced in the present study.

Another example of water soluble photo-curable chitosan is azidobenzoic acid-modified lactose chitosan (Az-CH-LA). However, Az-CH-LA synthesis requires a two-step condensation reaction to introduce the lactose and the azide moieties [90].

During chemical modification of gelatine, some conformational structures can be irreversibly altered, but MAG hydrogels are able to retain some important properties of gelatine, like cell adhesion domains, thermosensitivity and enzymatic degradability [91-93]. Through the chemical modification of gelatine and chitosan, the double bonds of the methacryl groups allowed hydrogels to be covalently crosslinked, using UV light in the presence of a photoinitiator [51, 79, 91]. Herein, Irgacue 2959 was used as the PI since it is soluble in water and is known for having minimal cytotoxicity over a broad range of mammalian cell types and species [52, 57]. Following the exposure of the precursor polymers solutions containing the PI, to UV light, the photoinitiator generates free radicals that initiate the polymerization process [43]. The reactive radicals will then attack the alkene groups of the incorporated methacrylamide resulting in crosslinked networks [47].

A macroscopic image of the produced 2:1 hydrogel is shown in figure 9. Photocrosslinkable MAC, MAG and MAC:MAG (2:1, 1:2, 1:2) hydrogels (6.5 mm x 6.5 mm x 1 mm) were produced by exposing the precursor polymer solutions to UV light (254 nm) for 20 and 10 min, respectively.

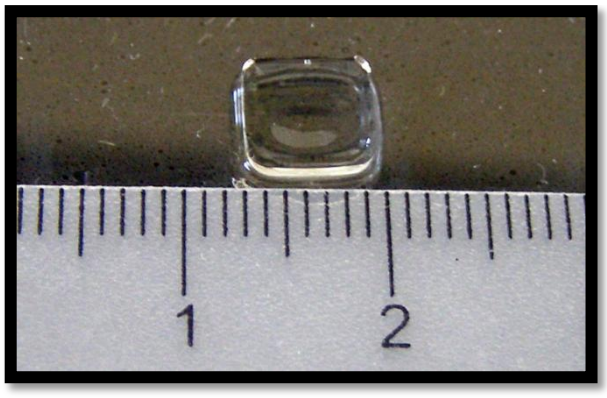

Figure 9: Macroscopic image of the 2:1 (MAC:MAG) photocrosslinkable hydrogel produced in this study.

The morphology and structure of hydrogels have a significant influence on the capacity of cells to infiltrate, adhere and proliferate, which ultimately affect its performance in tissue engineering [94].

In order to characterize the surface morphology and the cross-section structure of the photocrosslinkable hydrogels, SEM images of the lyophilized hydrogels were acquired (figure 10). The pore size varied with the ratio of MAC to MAG. As reported by Huang, herein it is also possible to observe that the addition of MAC allowed the formation of larger pores with an interconnected structure [73]. The hydrogel with the higher content of MAC (2:1) had larger pores, with an average size of 30 μm (determined using ImageJ software) and a highly porous inner structure. The interconnected and larger pores of this hydrogel are expected to allow an increased water uptake capacity, facilitating the diffusion of nutrients, biomolecules and cell waste products [94]. The 1:1 hydrogel had also a regular structure but with interconnected small pores at the surface, with an average size of 3 μm, and even smaller at the inside. The 1:2 hydrogel had an irregular surface with smaller pores, with an average size of 2 μm, and a more closed structure.

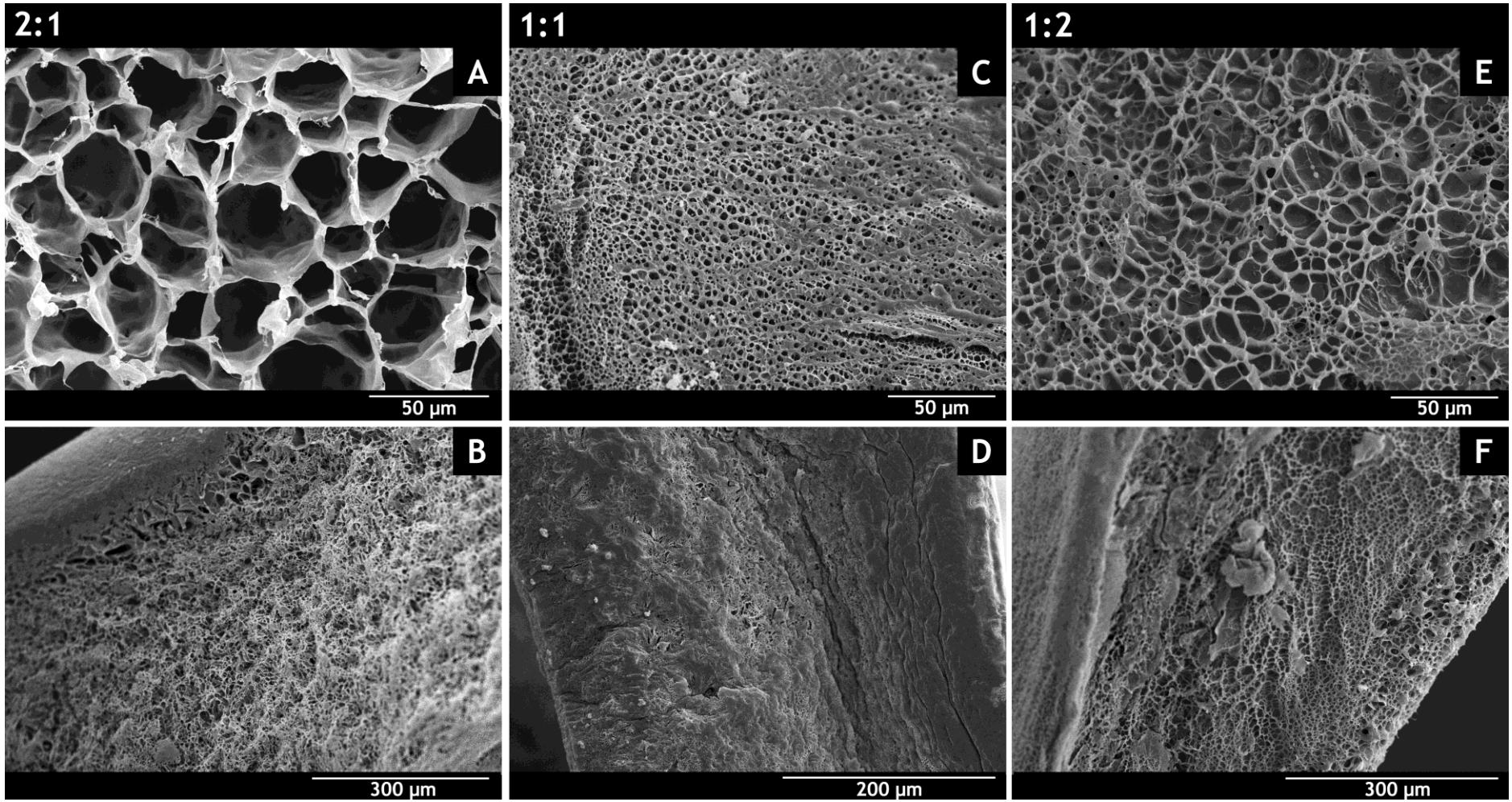

Figure 10: SEM images of MAC:MAG (2:1, 1:1, 1:2) hydrogels: A, C and E correspond to the surface of the 2:1, 1:1 and 1:2 hydrogels, respectively; B, D and F correspond to the cross-section of the 2:1, 1:1 and 1:2 hydrogels, respectively.

3.4. FTIR analysis of hydrogels

The FTIR analysis of the lyophilized hydrogels was performed to characterize the chemical composition of the different samples. FTIR spectra of all samples are presented in figure 11. The spectrum of the polymer MAC displayed bands at 3277, 2934 and 1652 cm^{-1} corresponding to the O-H stretch, C-H stretch and the C=O stretch of the MAC amide group, respectively. The absorption peaks at 1538 and 1062 cm^{-1} were assigned to the N-H stretch of the amide (II) group and to the C-O stretch, respectively [55, 94]. The spectrum of the polymer MAG, showed absorption bands at 3296 and 2938 cm^{-1} corresponding to the N-H stretch of amide (II) and C-H stretch, respectively. The peaks at 1633, 1540 and 1237 cm^{-1} were assigned to the C=O stretching vibrations of the MAG amide group, N-H bending vibrations of amide (II) and N-H bending of amide (III), respectively [70, 94]. The N-H stretch peak of MAC amide (II) and N-H bending vibration peak of MAG amide (II) were shifted to lower wavenumbers as the content of MAG increased.

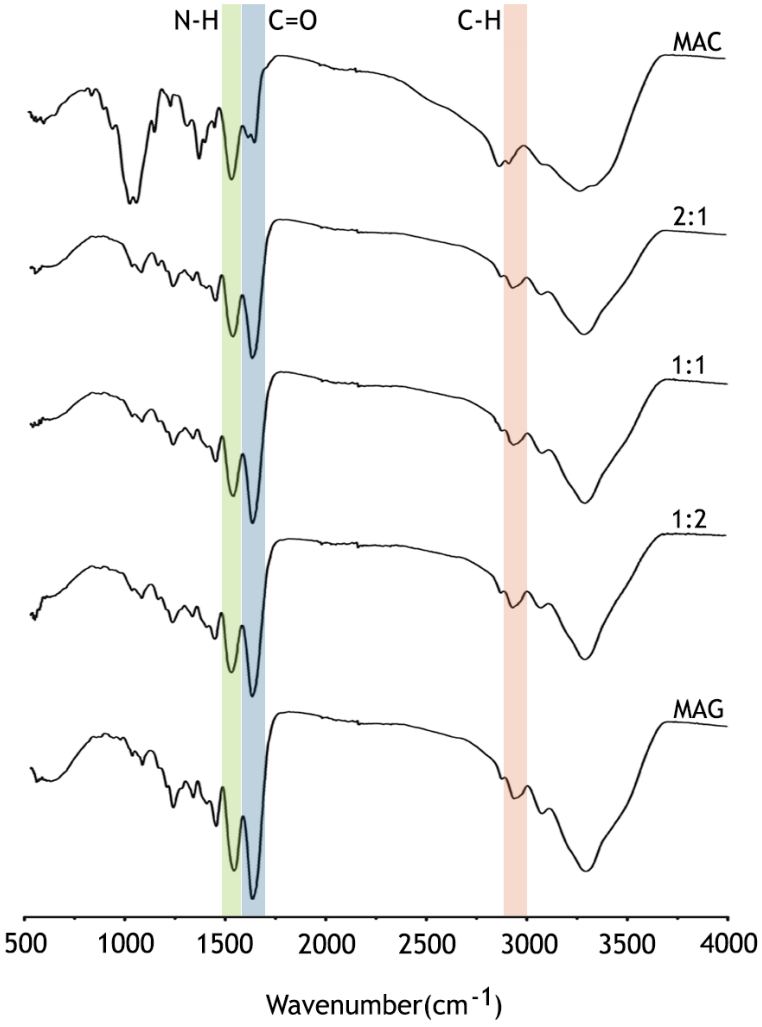

Figure 11: FTIR spectra of MAC and MAG polymers, and MAC:MAG (2:1, 1:1, 1:2) lyophilized hydrogels. The spectra of the MAC:MAG hydrogels are presented according to their decreased content of MAC.

3.5. Swelling profile of the hydrogels

The investigation of the swelling characteristics of MAC:MAG hydrogels is of great interest for wound dressing, since it evaluates their capacity to absorb wound exudates. The degree of swelling is dependent on the pore size of the polymeric network and on the polymer-solvent interactions [39, 91, 94].

The swelling behaviour of MAC:MAG (2:1, 1:1, 1:2) hydrogels is presented in figure 12. The results demonstrated that the produced hydrogels possess high water uptake capacity, specially the 2:1 hydrogel. As it is possible to observe, the maximum degree of swelling of the 2:1 and 1:1 hydrogels was reached during the first hour, while the 1:2 hydrogel reached its maximum after 3 h of incubation. Moreover, the swelling degree increased with the increase of the MAC content. Such swelling behaviour can be explained by the presence of hydrophilic groups in chitosan and gelatine, such as hydroxyl, amine and carboxyl groups that can be easily hydrated. The water uptake causes an increase of the pore diameters allowing a subsequent diffusion of cells, nutrients, bioactive molecules and waste products through the hydrogel, which is essential in skin regeneration [83].

Initially, the Tris-HCl solution diffused into the hydrogel matrices, leading to the hydrogel swelling before degradation. Polysaccharides are easily degraded by surrounding acids, alkalines or enzymes. Therefore, after the hydrogels reached the maximum degree of swelling, the rate of Tris-HCl diffusion into the hydrogel decreased, due to the collapse and degradation of the hydrogels [94]. The hydrogels degradation is beneficial since the lysozyme activity on chitosan will promote the proliferation of fibroblasts and afterwards result in the acceleration of wound healing and tissue regeneration [95].

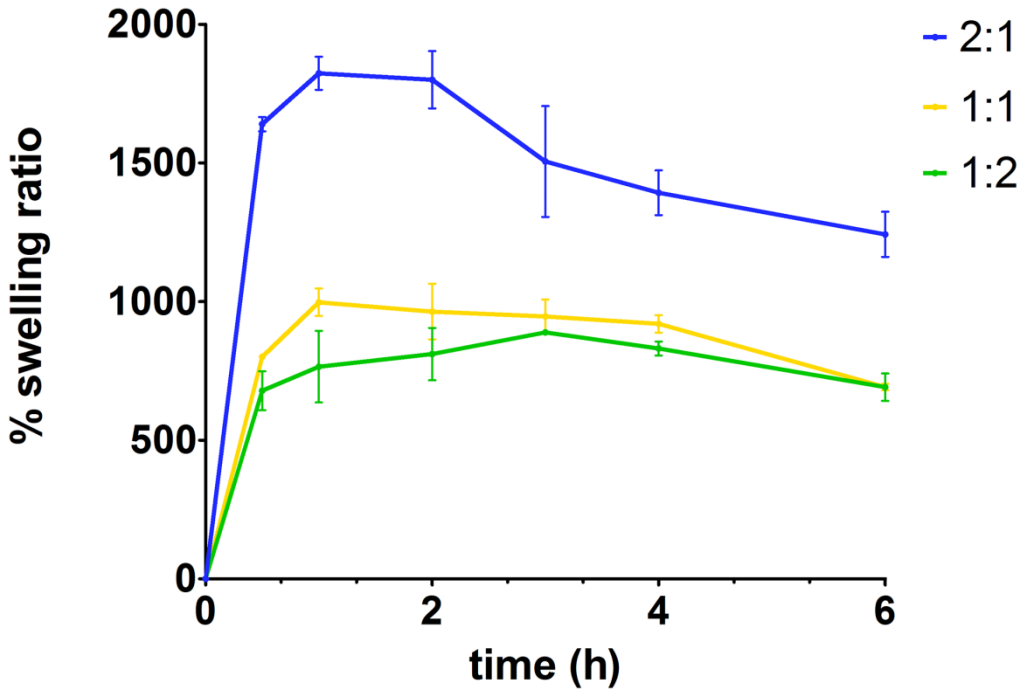

Figure 12: Swelling profile of the produced MAC:MAG (2:1, 1:1, 1:2) hydrogels.

3.6. Porosity evaluation

The porosity of the MAC:MAG hydrogels was performed through a liquid displacement method, using ethanol. The hydrogels porous structure support important functions in wound healing, like the promotion of drainage and gas exchange, and the prevention of exudates accumulation [22].

From the analysis of figure 13, it is possible to conclude that the 2:1 hydrogel presented the highest value of porosity (76% ± 0.8), when compared with the 1:1 (55% ± 1.7) and the 1:2 (44% ±1.6) hydrogels. Such results are in accordance with the data obtained through SEM analysis (figure 10). The porosity varied with the ratio of MAC to MAG. As reported by Huang, the addition of MAC allowed the formation of larger and interconnected pores and thus a more porous structure [73]. Moreover, the higher porosity of the 2:1 hydrogels also explains their increased swelling capacity. Therefore, the 2:1 hydrogels were expected to allow better cell migration, adhesion and proliferation and also the diffusion of nutrients, oxygen and waste products, leading to an improved wound healing.

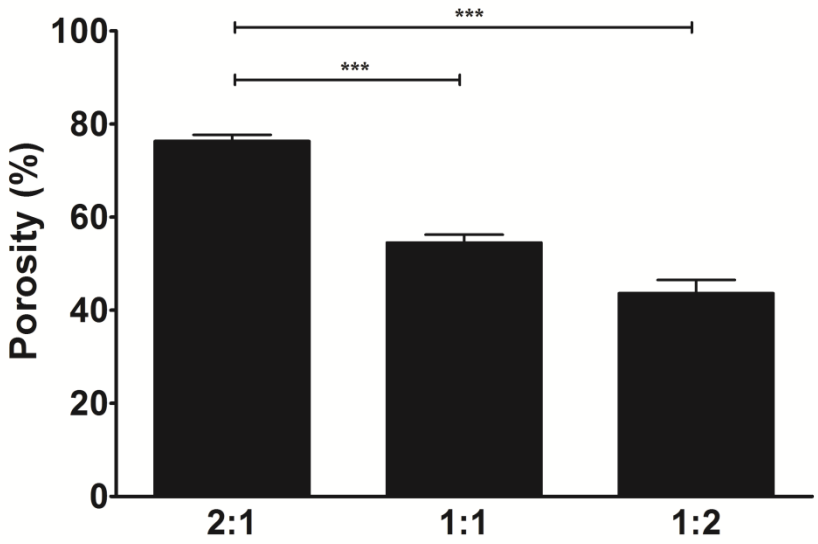

Figure 13: Porosity of the MAC:MAG (2:1, 1:1, 1:2) hydrogels. Statistical analysis was performed using one-way ANOVA with Newman-Keuls test (*** $p < 0.001$).

3.7. Characterization of the cytotoxic profile of the hydrogels

To evaluate the applicability of the produced hydrogels, as wound dressings, their cytocompatibility was characterized. NHDF were seeded in 96 well plates in contact with the materials and in their absence, for 24 and 72 h. The fibroblast cells were used due to their essential role in the wound healing process. Fibroblasts are involved in collagen synthesis and other components of ECM that allow wound healing [95].

Cell viability was quantitatively measured at 24 and 72 h using an MTS assay. MTS is a tetrazolium compound that is reduced, by mitochondrial activity of viable cells, into a water-soluble formazan product that can be measured at 492 nm. The MTS assay is a rapid, sensitive and specific method to evaluate materials cytotoxicity *in vitro* [96].

Initially, the cytocompatibility of the MAC and MAG hydrogels was evaluated in order to determine if the modified and crosslinked polymers caused any toxic effect. Since their biocompatibility was verified, the effect of the different ratios of MAC to MAG, on cells viability was also determined (figure 14).

As expected, the negative control (k^-), where cells were seeded just with DMEM-F12, showed about 100% of viable cells. In the positive control (k^+), where cells were treated with ethanol, almost no viable cells were observed. The MTS assay results showed a significant statistical

difference ($p < 0.001$) between the positive and negative controls and cells in contact with the hydrogels.

According to Gevaert *et al.*, cell viability is dependent on the hydrogel polymer concentration and thus on the network density and swelling properties [97]. Therefore the lower percentage of viable cells in MAG hydrogel when compared with MAC, can be correlated with the 10 times higher polymer concentration of MAG. Moreover, the MTS assay also showed that between the 24 and 72 h, cell viability increased in all the produced hydrogels and that only the 2:1 hydrogel presented a significant difference ($p < 0.001$) within this period. Despite RGD sequences of gelatine, that stimulate cell adhesion, chitosan free amine groups also promote cell proliferation [80, 83]. Previous studies showed that chitin-based dressings stimulate skin tissue regeneration by facilitating the contraction of wounds and regulating the secretion of inflammatory mediators [37]. Moreover, the highest porosity of the 2:1 hydrogel, might have also promoted the diffusion of nutrients and cells waste products, and therefore improved cell proliferation and survival.

Therefore, it was possible to conclude that from the MAC:MAG hydrogels, the hydrogel with more chitosan content (2:1) was the only one that significantly improved the fibroblast cells proliferation and might be the most suitable for being used with wound healing purposes.

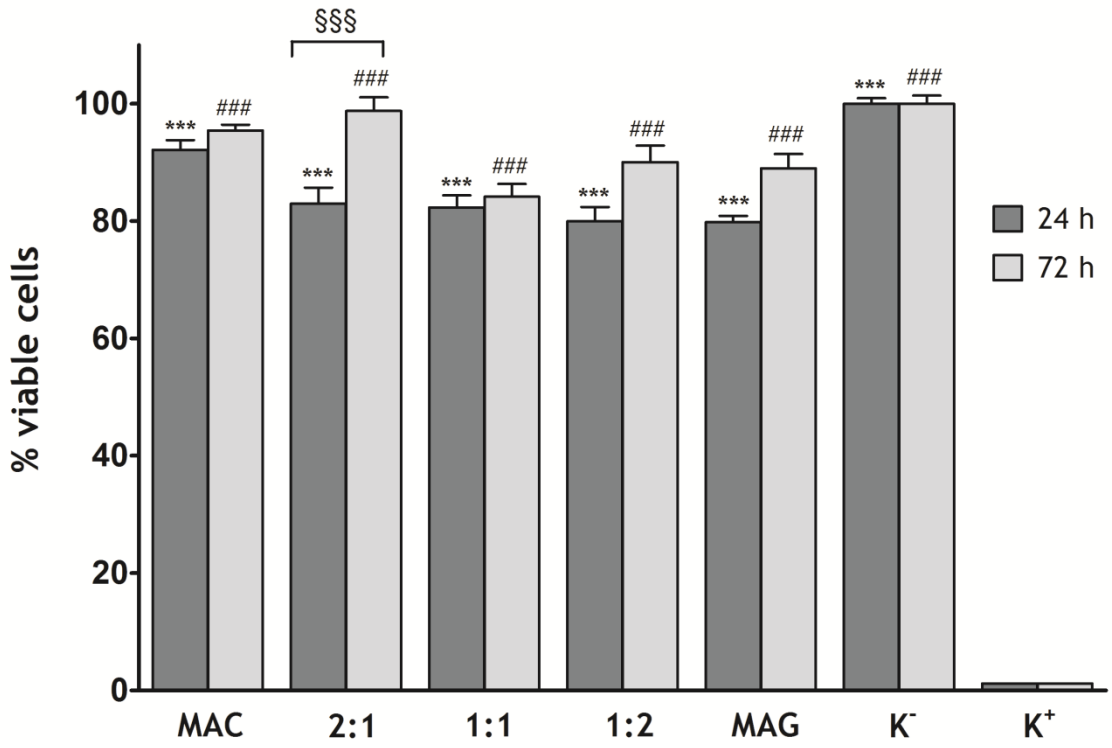

Figure 14: Evaluation of cellular viability through an MTS assay, after 24 and 72 h. K^+ (dead cells); K^- (live cells); MAC (methacrylamide chitosan); MAG (methacrylamide gelatine); 2:1, 1:1 and 1:2 referred to MAC:MAG volume ratios. Each result is the mean ± standard error of the mean of at least three independent experiments. Statistical analysis was performed using one-way ANOVA with Dunnet's post hoc test and Newman-Keuls multiple comparison test (***, # # #, §§§, $p < 0.001$).

3.8. Evaluation of cell proliferation in the presence of hydrogels

The ability of cells to attach to hydrogels' surface is essential for biomedical applications [91]. Therefore, cell adhesion and proliferation in contact with the hydrogels were evaluated. Only the MAC:MAG hydrogels at the different ratios were tested. For that, NHDF were also seeded in 96 well plates with or without the hydrogels.

At predetermined time intervals, cell adhesion and proliferation were observed using an inverted light microscope. Figure 15 shows that in the negative control (K^-) and wells where cells were in contact with hydrogels, cells adhered and remained viable, being possible to observe their spreading and elongation. In the positive control (K^+), dead cells with a typical spherical shape were visualized.

To better characterize the influence of MAC:MAG (2:1, 1:1, 1:2) hydrogels' surface on cell adhesion, SEM analysis was also performed (figure 16). After 24 h in contact with this hydrogels, fibroblasts were already attached and highly spread. After 72 h, fibroblasts were even more spread and also started to form a continuous layer of cells.

The interaction between 3D polymeric matrices and cells is mediated by integrins, which recognize specific motifs at materials' surface and allow physical anchoring. This process comprises a cascade of four events: cell attachment, cell spreading, organization of actin cytoskeleton and formation of focal adhesions [98]. The hydrogel with the higher content of gelatine (1:2) was the one that seemed to present the most spread fibroblasts. This is in accordance with Huang which reported that cells were more spread in gelatine hydrogels than in the chitosan-gelatine ones [73]. Such can be attributed to the RGD sequence content of gelatine that is known for being the most effective peptide sequence to stimulate cell adhesion on materials surface [80, 98].

The results obtained demonstrated that the produced photocrosslinkable hydrogels are biocompatible, promote cell adhesion and proliferation along time and therefore they might be suitable for skin regeneration.

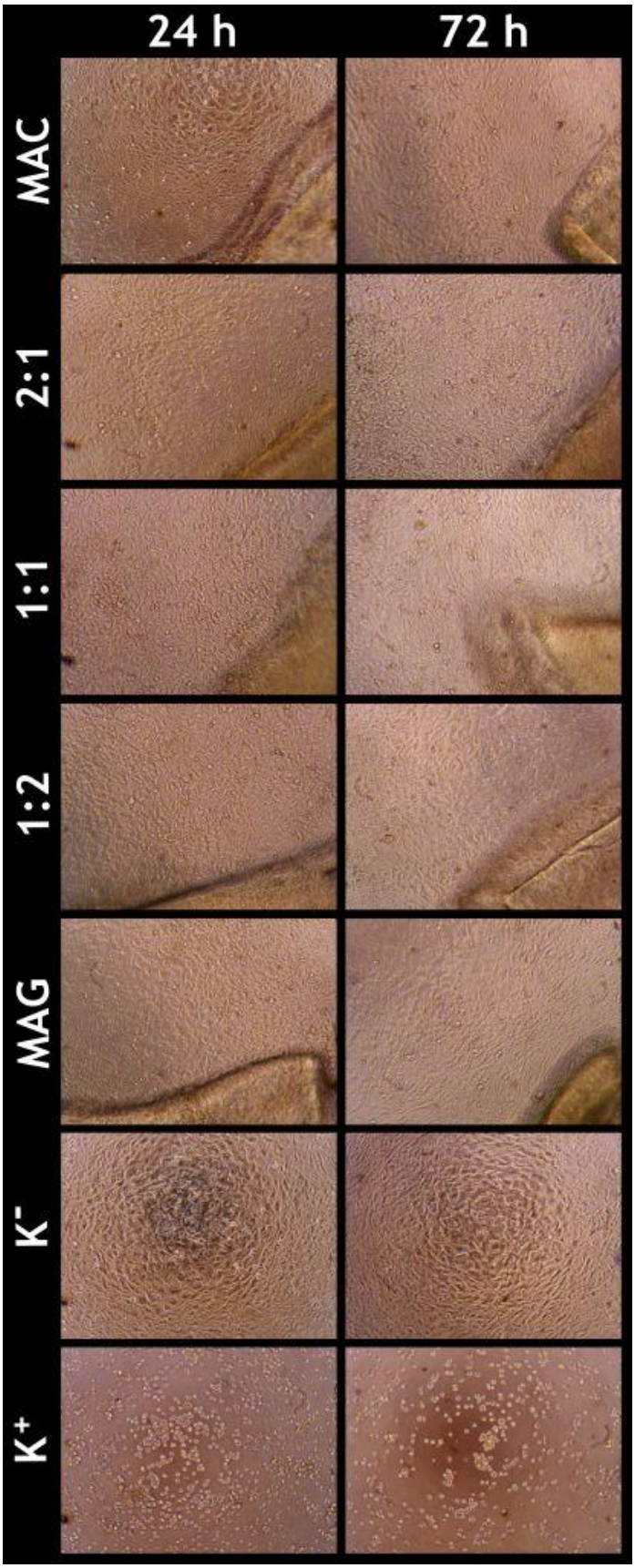

Figure 15: Microscopic images of NHDF cells after 24 and 72 h in contact with MAC, MAG and MAC:MAG (2:1, 1:1, 1:2) hydrogels; positive control (K^+); negative control (K^-).

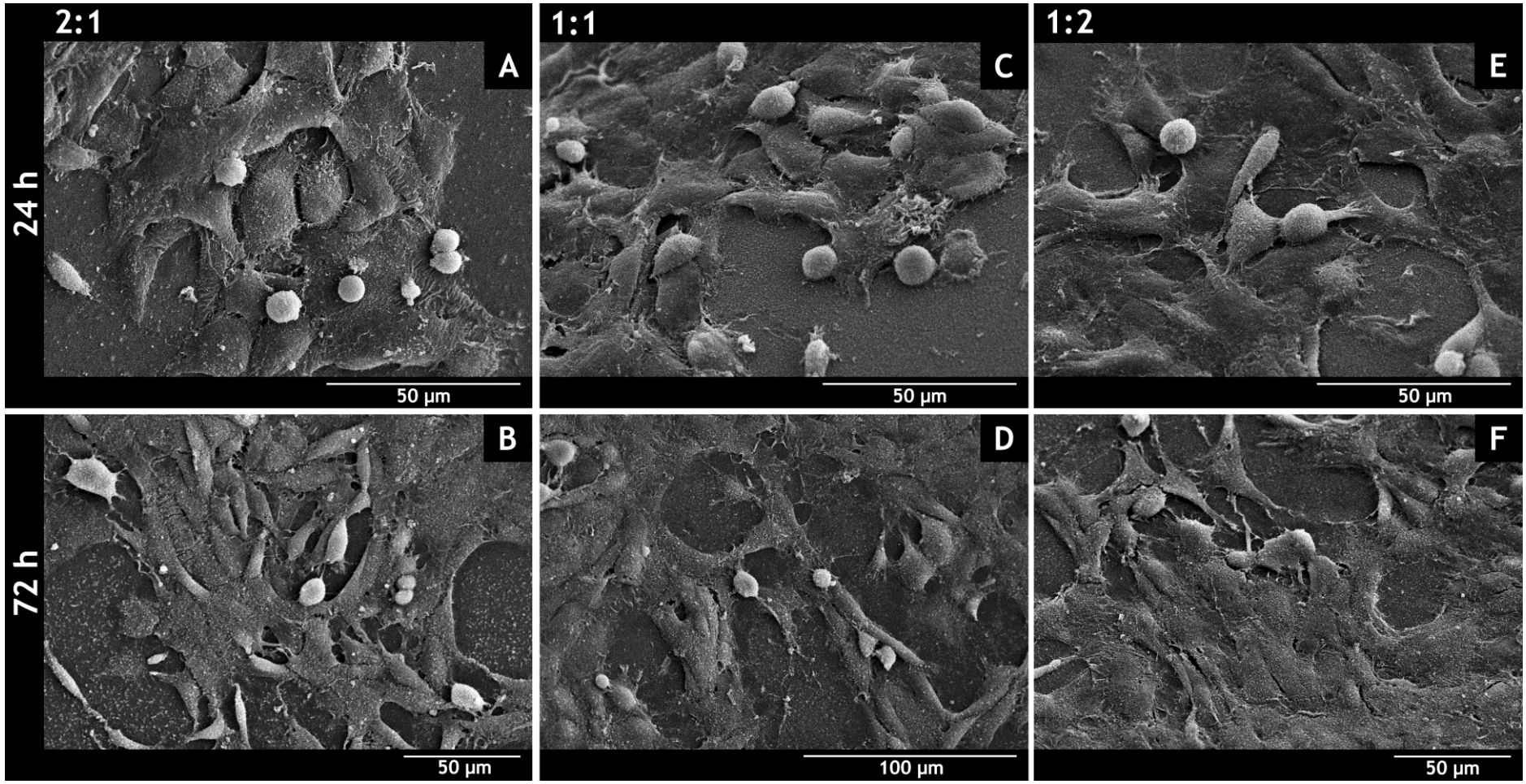

Figure 16: SEM images of NHDF cells in contact with MAC:MAG (2:1, 1:1, 1:2) hydrogels. A, C and E correspond to images of cells on top of 2:1, 1:1 and 1:2 hydrogels after 24 h and B, D, F correspond to 2:1, 1:1 and 1:2 after 72 h.

Chapter IV

Conclusion and Future Perspectives

4. Conclusion and Future Perspectives

Every day skin lesions affect people worldwide and some of them can severely compromise the patient health. In order to surpass this health problem and enhance the wound healing process, several therapeutic approaches have been developed. Among the different available products, hydrogels stand out due to their capacity to mimic the ECM. These 3D matrices have high permeability to gases, nutrients and waste products and allow cell adhesion and proliferation.

In the present work, chitosan and gelatine primary amine groups were modified through the incorporation of methacrylate groups, leading to the synthesis of MAC and MAG. The degree of modification, 33% and 23%, respectively, was determined by proton nuclear magnetic resonance. The precursor MAC and MAG solutions were blended at different ratios and their exposure to UV light, in the presence of a photoinitiator, allowed the production of the hydrogels.

The chemical composition and the structure of the MAC:MAG hydrogels at different ratios (2:1, 1:1 and 1:2) was characterized by FTIR and SEM analysis. FTIR analysis indicated that the blend of the two polymers was successfully achieved. The SEM images of the hydrogels showed that the hydrogel 2:1, with higher chitosan content, had the most porous and interconnected structure, with larger pore sizes. This porous network also revealed to have a better water uptake capacity.

The cytotoxic profile of all the hydrogels was assessed through an MTS assay and the results confirmed that they were not toxic for fibroblast cells. Moreover, the hydrogels with greater MAC content had a higher percentage of viable cells. According to SEM images of the MAC:MAG hydrogels in the presence of fibroblasts, they were also able to support cell adhesion and proliferation on their surface.

The results indicate that the produced hydrogels have suitable physical and biological properties that support their future applicability as wound dressings. The produced hydrogels can be lyophilised in order to be stored and thus be ready for use, while maintaining their intrinsic properties.

In a near future, *in vivo* assays will be performed to evaluate the local and systemic histocompatibility of the MAC:MAG hydrogels and also their capacity to improve the wound healing process. Moreover, growth factors and antimicrobial agents can be incorporated in the hydrogels in order to improve wound repair and prevent bacterial infections, respectively.

Chapter V

References

5. References

1. Marieb, E.N. and K. Hoehn, *Human anatomy & physiology* 7th ed. 2007: Pearson Education.

2. Lei, P., H. You, and S.T. Andreadis, *Organ Regeneration*. 2013: Springer.

3. Clark, R.A.F., K. Ghosh, and M.G. Tonnesen, *Tissue engineering for cutaneous wounds*. Journal of Investigative Dermatology, 2007. **127**(5): p. 1018-1029.

4. Kondo, T. and Y. Ishida, *Molecular pathology of wound healing*. Forensic science international, 2010. **203**(1-3): p. 93-8.

5. Ajani, G., et al., *Cellular responses to disruption of the permeability barrier in a three-dimensional organotypic epidermal model*. Experimental cell research, 2007. **313**(14): p. 3005-3015.

6. Yildirimer, L., N.T. Thanh, and A.M. Seifalian, *Skin regeneration scaffolds: a multimodal bottom-up approach*. Trends in biotechnology, 2012. **30**(12): p. 638-648.

7. Sachs, D.L. and J.J. Voorhees, *Age-reversing drugs and devices in dermatology*. Clinical pharmacology and therapeutics, 2011. **89**(1): p. 34-43.

8. Metcalfe, A.D. and M.W. Ferguson, *Tissue engineering of replacement skin: the crossroads of biomaterials, wound healing, embryonic development, stem cells and regeneration*. Journal of the Royal Society, Interface, 2007. **4**(14): p. 413-437.

9. Brohem, C.A., et al., *Artificial skin in perspective: concepts and applications*. Pigment cell & melanoma research, 2011. **24**(1): p. 35-50.

10. Zhang, Z. and B.B. Michniak-Kohn, *Tissue engineered human skin equivalents*. Pharmaceutics, 2012. **4**(1): p. 26-41.

11. Mescher, A.L. and L.C. Junqueira, *Junqueira's Basic Histology: Text & Atlas* 12th ed. 2010: Mcgraw-hill medical New York.

12. Candi, E., R. Schmidt, and G. Melino, *The cornified envelope: a model of cell death in the skin*. Nature reviews Molecular cell biology, 2005. **6**(4): p. 328-340.

13. Fuchs, E., *Finding one's niche in the skin*. Cell Stem Cell, 2009. **4**(6): p. 499-502.

14. Seeley, R., T. Stephens, and P. Tate, *Anatomy & physiology* 6th ed. 2005.

15. MacNeil, S., *Biomaterials for tissue engineering of skin*. Materials today, 2008. **11**(5): p. 26-35.

16. Boateng, J.S., et al., *Wound healing dressings and drug delivery systems: a review*. Journal of pharmaceutical sciences, 2008. **97**(8): p. 2892-2923.

17. Shevchenko, R.V., S.L. James, and S.E. James, *A review of tissue-engineered skin bioconstructs available for skin reconstruction.* Journal of the Royal Society, Interface 2010. **7**(43): p. 229-258.

18. Ribeiro, M.P., et al., *Dextran-based hydrogel containing chitosan microparticles loaded with growth factors to be used in wound healing.* Materials Science and Engineering: C, 2013. **33**(5): p. 2958-2966.

19. Li, J., J. Chen, and R. Kirsner, *Pathophysiology of acute wound healing.* Clinics in dermatology, 2007. **25**(1): p. 9-18.

20. Enoch, S. and D.J. Leaper, *Basic science of wound healing.* Surgery (Oxford), 2008. **26**(2): p. 31-37.

21. Beldon, P., *Basic science of wound healing.* Surgery (Oxford), 2010. **28**(9): p. 409-412.

22. Ribeiro, M.P., et al., *Development of a new chitosan hydrogel for wound dressing.* Wound Repair Regen, 2009. **17**(6): p. 817-824.

23. Auger, F.A., D. Lacroix, and L. Germain, *Skin substitutes and wound healing.* Skin Pharmacology and Physiology, 2009. **22**(2): p. 94-102.

24. Gurtner, G.C., et al., *Wound repair and regeneration.* Nature, 2008. **453**(7193): p. 314-321.

25. Singer, A.J. and R.A.F. Clark, *Skin and Soft Tissue Injuries and Infections: A Practical Evidence Based Guide,* 2010: People's Medical Publisinhing House.

26. Pereira, R.F., et al., *Advanced biofabrication strategies for skin regeneration and repair.* Nanomedicine, 2013. **8**(4): p. 603-621.

27. Shakespeare, P.G., *The role of skin substitutes in the treatment of burn injuries.* Clinics in dermatology, 2005. **23**(4): p. 413-418.

28. Atiyeh, B.S., S.N. Hayek, and S.W. Gunn, *New technologies for burn wound closure and healing--review of the literature.* Burns : journal of the International Society for Burn Injuries, 2005. **31**(8): p. 944-956.

29. Bronzino, J.D., *Biomedical engineering handbook*. Vol. 1. 1999: CRC press.

30. Dvir, T., et al., *Nanotechnological strategies for engineering complex tissues.* Nature nanotechnology, 2011. **6**(1): p. 13-22.

31. Nair, L.S. and C.T. Laurencin. Tissue engineering I. 2006: Springer.

32. Bottcher-Haberzeth, S., T. Biedermann, and E. Reichmann, *Tissue engineering of skin.* Burns : journal of the International Society for Burn Injuries, 2010. **36**(4): p. 450-460.

33. MacNeil, S., *Progress and opportunities for tissue-engineered skin.* Nature, 2007. **445**(7130): p. 874-880.

34. Queen, D., et al., *A dressing history*. International wound journal, 2004. **1**(1): p. 59-77.

35. Falabella, A.F., *Debridement and wound bed preparation*. Dermatologic therapy, 2006. **19**(6): p. 317-325.

36. Huang, X., et al., *Influence of radiation crosslinked carboxymethyl-chitosan/gelatin hydrogel on cutaneous wound healing*. Materials science & engineering. C, Materials for biological applications, 2013. **33**(8): p. 4816-4824.

37. Jayakumar, R., et al., *Biomaterials based on chitin and chitosan in wound dressing applications*. Biotechnology advances, 2011. **29**(3): p. 322-337.

38. Anthony, E.T., et al., *The development of novel dermal matrices for cutaneous wound repair*. Drug Discovery Today: Therapeutic Strategies, 2006. **3**(1): p. 81-86.

39. Mihaila, S.M., et al., *Photocrosslinkable kappa-carrageenan hydrogels for tissue engineering applications*. Advanced healthcare materials, 2013. **2**(6): p. 895-907.

40. Nguyen, K.T. and J.L. West, *Photopolymerizable hydrogels for tissue engineering applications*. Biomaterials, 2002. **23**(22): p. 4307-4314.

41. Shin, H., B.D. Olsen, and A. Khademhosseini, *The mechanical properties and cytotoxicity of cell-laden double-network hydrogels based on photocrosslinkable gelatin and gellan gum biomacromolecules*. Biomaterials, 2012. **33**(11): p. 3143-3152.

42. Mironi-Harpaz, I., et al., *Photopolymerization of cell-encapsulating hydrogels: crosslinking efficiency versus cytotoxicity*. Acta biomaterialia, 2012. **8**(5): p. 1838-1848.

43. Jeon, O., et al., *Photocrosslinked alginate hydrogels with tunable biodegradation rates and mechanical properties*. Biomaterials, 2009. **30**(14): p. 2724-2734.

44. Huang, S. and X. Fu, *Naturally derived materials-based cell and drug delivery systems in skin regeneration*. Journal of controlled release, 2010. **142**(2): p. 149-159.

45. Coutinho, D.F., et al., *Modified Gellan Gum hydrogels with tunable physical and mechanical properties*. Biomaterials, 2010. **31**(29): p. 7494-7502.

46. Drury, J. and D. Mooney, *Hydrogels for tissue engineering: scaffold design variables and applications*. Biomaterials, 2003. **24**(24): p. 4337-4351.

47. Annabi, N., et al., *25th Anniversary Article: Rational Design and Applications of Hydrogels in Regenerative Medicine*. Advanced Materials Research, 2014. **26**(1): p. 85-124.

48. Hoffman, A.S., *Hydrogels for biomedical applications*. Advanced drug delivery reviews, 2012. **64**: p. 18-23.

49. Xiao, W., et al., *Synthesis and characterization of photocrosslinkable gelatin and silk fibroin interpenetrating polymer network hydrogels*. Acta biomaterialia, 2011. **7**(6): p. 2384-2393.

50. Kim, S., et al., *In vitro evaluation of photo-crosslinkable chitosan-lactide hydrogels for bone tissue engineering.* Journal of biomedical materials research. Part B, Applied biomaterials, 2014: p. 1393–1406.

51. Levett, P.A., et al., *Chondrocyte redifferentiation and construct mechanical property development in single-component photocrosslinkable hydrogels.* Journal of biomedical materials research. Part A, 2014. **102**(8): p. 2544-2553.

52. Williams, C.G., et al., *Variable cytocompatibility of six cell lines with photoinitiators used for polymerizing hydrogels and cell encapsulation.* Biomaterials, 2005. **26**(11): p. 1211-1218.

53. Zhong, C., et al., *Synthesis, characterization and cytotoxicity of photo-crosslinked maleic chitosan-polyethylene glycol diacrylate hybrid hydrogels.* Acta biomaterialia, 2010. **6**(10): p. 3908-3918.

54. Tsai, B., C. Lin, and J. Lin, *Synthesis and property evaluations of photocrosslinkable chitosan derivative and its photocopolymerization with poly (ethylene glycol).* Journal of applied polymer science, 2006. **100**(3): p. 1794-1801.

55. Monier, M., et al., *Synthesis and characterization of photo-crosslinkable hydrogel membranes based on modified chitosan.* Polymer, 2010. **51**(5): p. 1002-1009.

56. Ferreira, P., et al., *Biomedical Engineering - Frontiers and Challenges,* 2011: InTech.

57. Bryant, S.J., C.R. Nuttelman, and K.S. Anseth, *Cytocompatibility of UV and visible light photoinitiating systems on cultured NIH/3T3 fibroblasts in vitro.* Journal of Biomaterials Science, Polymer Edition, 2000. **11**(5): p. 439-457.

58. Gao, X., et al., *A water-soluble photocrosslinkable chitosan derivative prepared by Michael-addition reaction as a precursor for injectable hydrogel.* Carbohydrate Polymers, 2010. **79**(3): p. 507-512.

59. Lin, R.Z., et al., *Transdermal regulation of vascular network bioengineering using a photopolymerizable methacrylated gelatin hydrogel.* Biomaterials, 2013. **34**(28): p. 6785-6796.

60. Ishihara, M., et al., *Photocrosslinkable chitosan as a dressing for wound occlusion and accelerator in healing process.* Biomaterials, 2002. **23**(3): p. 833-840.

61. Fujita, M., et al., *Efficacy of photocrosslinkable chitosan hydrogel containing fibroblast growth factor-2 in a rabbit model of chronic myocardial infarction.* The journal of surgical research, 2005. **126**(1): p. 27-33.

62. Dodane, V. and V.D. Vilivalam, *Pharmaceutical applications of chitosan.* Pharmaceutical Science & Technology Today, 1998. **1**(6): p. 246-253.

63. Bhat, S., A. Tripathi, and A. Kumar, *Supermacroprous chitosan-agarose-gelatin cryogels: in vitro characterization and in vivo assessment for cartilage tissue engineering.* Journal of the Royal Society Interface, 2011. **8**(57): p. 540-554.

64. Malafaya, P.B., G.A. Silva, and R.L. Reis, *Natural-origin polymers as carriers and scaffolds for biomolecules and cell delivery in tissue engineering applications.* Advanced drug delivery reviews, 2007. **59**(4-5): p. 207-233.

65. Dash, M., et al., *Chitosan—A versatile semi-synthetic polymer in biomedical applications.* Progress in Polymer Science, 2011. **36**(8): p. 981-1014.

66. Yu, L.M., K. Kazazian, and M.S. Shoichet, *Peptide surface modification of methacrylamide chitosan for neural tissue engineering applications.* J Biomed Mater Res A, 2007. **82**(1): p. 243-55.

67. Kim, I.Y., et al., *Chitosan and its derivatives for tissue engineering applications.* Biotechnology advances, 2008. **26**(1): p. 1-21.

68. Jayakumar, R., et al., *Biomedical applications of chitin and chitosan based nanomaterials—A short review.* Carbohydrate Polymers, 2010. **82**(2): p. 227-232.

69. Peng, Z., Z. Peng, and Y. Shen, *Fabrication and properties of gelatin/chitosan composite hydrogel.* Polymer-Plastics Technology and Engineering, 2011. **50**(11): p. 1160-1164.

70. Sarem, M., et al., *Optimization strategies on the structural modeling of gelatin/chitosan scaffolds to mimic human meniscus tissue.* Materials science & engineering. C, Materials for biological applications, 2013. **33**(8): p. 4777-4785.

71. Abuknesha, R.A., et al., *Detection of proteases using an immunochemical method with haptenylated-gelatin as a solid-phase substrate.* Analytical and bioanalytical chemistry, 2010. **396**(7): p. 2547-2558.

72. Hoch, E., et al., *Stiff gelatin hydrogels can be photo-chemically synthesized from low viscous gelatin solutions using molecularly functionalized gelatin with a high degree of methacrylation.* Journal of materials science. Materials in medicine, 2012. **23**(11): p. 2607-2617.

73. Huang, Y., et al., *In vitro characterization of chitosan-gelatin scaffolds for tissue engineering.* Biomaterials, 2005. **26**(36): p. 7616-7627.

74. Gómez-Guillén, M.C., et al., *Functional and bioactive properties of collagen and gelatin from alternative sources: A review.* Food Hydrocolloids, 2011. **25**(8): p. 1813-1827.

75. Dubruel, P., et al., *Porous gelatin hydrogels: 2. In vitro cell interaction study.* Biomacromolecules, 2007. **8**(2): p. 338-344.

76. Rose, J.B., et al., *Gelatin-Based Materials in Ocular Tissue Engineering.* Materials, 2014. **7**(4): p. 3106-3135.

77. Gaspar, V.M., et al., *Formulation of chitosan-TPP-pDNA nanocapsules for gene therapy applications.* Nanotechnology, 2011. **22**(1): p. 015101.

78. Muzzarelli, R.A.A. and R. Rocchetti, *Determination of the degree of acetylation of chitosans by first derivative ultraviolet spectrophotometry.* Carbohydrate Polymers, 1985. **5**(6): p. 461-472.

79. Yu, L.M., K. Kazazian, and M.S. Shoichet, *Peptide surface modification of methacrylamide chitosan for neural tissue engineering applications.* Journal of biomedical materials research. Part A, 2007. **82**(1): p. 243-255.

80. Hoch, E., et al., *Chemical tailoring of gelatin to adjust its chemical and physical properties for functional bioprinting.* Journal of Materials Chemistry B, 2013. **1**(41): p. 5675-5685.

81. Gulrez, S.K.H., S. Al-Assaf, and G.O. Phillips, *Hydrogels: methods of preparation, characterisation and applications.* Progress in Molecular and Environmental Bioengineering-From Analysis and Modeling to Technology pplications, 2011: p. 117-150.

82. Correia, T.R., et al., *A bi-layer electrospun nanofiber membrane for plasmid DNA recovery from fermentation broths.* Separation and Purification Technology, 2013. **112**: p. 20-25.

83. Miguel, S.P., et al., *Thermoresponsive chitosan-agarose hydrogel for skin regeneration.* Carbohydrate polymers, 2014. **111**: p. 366-373.

84. Oliveira, M.B., et al., *In vivo high-content evaluation of three-dimensional scaffolds biocompatibility.* Tissue Engineering Part C: Methods, 2014.

85. Cha, C., et al., *Structural Reinforcement of Cell-Laden Hydrogels with Microfabricated Three Dimensional Scaffolds.* Biomaterials science, 2014. **2**(5): p. 703-709.

86. Yuan, Y., et al., *Deacetylation of chitosan: Material characterization and in vitro evaluation via albumin adsorption and pre-osteoblastic cell cultures.* Materials, 2011. **4**(8): p. 1399-1416.

87. Valmikinathan, C.M., et al., *Photocrosslinkable chitosan based hydrogels for neural tissue engineering.* Soft Matter, 2012. **8**(6): p. 1964-1976.

88. Brinkman, W.T., et al., *Photo-cross-linking of type I collagen gels in the presence of smooth muscle cells: mechanical properties, cell viability, and function.* Biomacromolecules, 2003. **4**(4): p. 890-895.

89. Li, H., A. Wijekoon, and N.D. Leipzig, *3D differentiation of neural stem cells in macroporous photopolymerizable hydrogel scaffolds.* PLoS One, 2012. **7**(11): p. e48824.

90. Ta, H.T., C.R. Dass, and D.E. Dunstan, *Injectable chitosan hydrogels for localised cancer therapy.* Journal of controlled release, 2008. **126**(3): p. 205-216.

91. Nichol, J.W., et al., *Cell-laden microengineered gelatin methacrylate hydrogels.* Biomaterials, 2010. **31**(21): p. 5536-5544.

92. Van Den Bulcke, A.I., et al., *Structural and rheological properties of methacrylamide modified gelatin hydrogels.* Biomacromolecules, 2000. **1**(1): p. 31-38.

93. Benton, J.A., et al., *Photocrosslinking of gelatin macromers to synthesize porous hydrogels that promote valvular interstitial cell function.* Tissue Engineering Part A, 2009. **15**(11): p. 3221-3230.

94. Yang, C., et al., *A green fabrication approach of gelatin/CM-chitosan hybrid hydrogel for wound healing.* Carbohydrate Polymers, 2010. **82**(4): p. 1297-1305.

95. Chen, Y.C., et al., *Functional Human Vascular Network Generated in Photocrosslinkable Gelatin Methacrylate Hydrogels.* Advanced functional materials, 2012. **22**(10): p. 2027-2039.

96. Malich, G., B. Markovic, and C. Winder, *The sensitivity and specificity of the MTS tetrazolium assay for detecting the in vitro cytotoxicity of 20 chemicals using human cell lines.* Toxicology, 1997. **124**(3): p. 179-192.

97. Gevaert, E., et al., *Galactose-functionalized gelatin hydrogels improve the functionality of encapsulated HepG2 cells.* Macromolecular bioscience, 2014. **14**(3): p. 419-427.

98. Hersel, U., C. Dahmen, and H. Kessler, *RGD modified polymers: biomaterials for stimulated cell adhesion and beyond.* Biomaterials, 2003. **24**(24): p. 4385-4415.